# MULTI-BODY INTERACTIONS IN COARSE-GRAINING SCHEMES FOR EXTENDED SYSTEMS

SASANKA ARE*, MARKOS A. KATSOULAKIS†, PETR PLECHÁČ‡, AND LUC REY-BELLET§

**Abstract.** In [12, 14] coarse-graining schemes for stochastic many body microscopic models focusing on equilibrium stochastic lattice systems were developed and furthermore, the accuracy of the coarse-graining schemes was estimated in terms of information loss between the exact and approximate coarse-grained Gibbs measures. The relative entropy estimates are given in terms of a small parameter $\epsilon$. In this paper we focus on the error quantification of the coarse-graine approximation and identifying the parameter $\epsilon$ based on the dependence on the underlying potential. In particular we study the role of multi-body interactions which are often not included in coarse-graining schemes as they can be computational expensive. The derived error estimates suggests strategies to overcome the computational expense due to the inclusion of multi-body interactions by either (a) truncating the multi-body interactions or by (b) splitting the potential into a short range piece where multi-body interactions are necessary and a smooth long range component where two-body interactions are sufficient. We present numerical examples that demonstrate that the inclusion of multi-body interactions shows substantial improvement in the dynamics even in regimes where the effect of multi-body interactions in predicting equilibrium properites is minimal, see [14]. We conclude with a detailed discussion on the relevance and impact of the multi-body interactions in off-lattice sytems.

**Key words.** coarse-graining, a posteriori error estimate, adaptivity, relative entropy, lattice spin systems, Monte Carlo method, Gibbs measure, cluster expansion, renormalization group map.

**AMS subject classifications.** 65C05, 65C20, 82B20, 82B80, 82-08

## 1. Introduction.

Molecular Dynamics (MD) or Monte Carlo (MC) methods have been used to simulate microscopic systems with complex interactions in a broad spectrum of scientific disciplines. However, one of the main hurdles in the computations with such methods is the computational difficulties that arise in simulating such molecular systems for spatio-temporal scales of realistic size. A class of computational tools that has been developed in the recent years in the physics, applied sciences and engineering literatures, in order to bridge such scale gaps by speeding-up microscopic simulation methods, is the method of coarse-graining.

Coarse-grained models, when compared to original microscopic systems, have fewer observables while at the same time are expected to describe accurately the unresolved degrees of freedom through a proper inclusion of stochastic fluctuations. In particular, in polymer science a sophisticated array of methods have been developed grouping systematically several atoms on a macromolecule creating an effective new chain[2, 5, 7, 22] Such coarse-graining strategies are designed to describe the complex microscopic short and long range interactions at the coarse-grained level while making a few adhoc assumptions. For example in coarse-grained united atom models [5], the coarse interactions between two macromolecules are assumed to be independent of the rest of the molecules/atoms in the polymer chain, in essence eliminating multi-body interactions of the coarse-grained potential. In fact, one of the main focus points of this paper is to address the role of the multi-body interactions in coarse-graining. In

*Department of Mathematics, University of Massachusetts (are@math.umass.edu).
†Department of Mathematics, University of Massachusetts (markos@math.umass.edu).
‡Mathematics Institute, University of Warwick (plechac@maths.warwick.ac.uk).
§Department of Mathematics, University of Massachusetts(luc@math.umass.edu).

particular, in Sect.6, we discuss specifically the relation between the coarse-graining of the united atom model and the coarse-graining schemes presented here.

The coarse-graining studied in this paper is based on the coarse-graining schemes for stochastic lattice systems such as Ising-type model that were developed in [14]. We consider stochastic lattice systems such as Ising-type because they are technically much simpler than off-lattice models, while they incorporate all important features of the problem. This class of stochastic lattice processes is employed in the modeling of adsorption, desorption, reaction and diffusion of chemical species in numerous applied science areas such as catalysis, microporous materials, biological systems. etc.

The microscopic system consists of a periodic lattice $\Lambda_N$, at each $x \in \Lambda_N$ we define an order parameter $\sigma(x)$; for instance, when taking values 0 and 1, it can describe vacant and occupied sites. The energy $H_N(\sigma)$ of the system, at the configuration $\sigma = \{\sigma(x) : x \in \Lambda_N\}$, is given by the Hamiltonian,

$$H_N(\sigma) = -\frac{1}{2}\sum_{x\in\Lambda_N}\sum_{y\neq x} J(x-y)\sigma(x)\sigma(y) + \sum_{x\in\Lambda_N} h(x)\sigma(x)\,, \tag{1.1}$$

where $h$, is the external field and $J$ is the interparticle potential. Equilibrium states at temperature $T$ are described by the (canonical) Gibbs measure,

$$\mu_{N,\beta}(d\sigma) = {Z_N}^{-1} e^{-\beta H_N(\sigma)} P_N(d\sigma)\,, \tag{1.2}$$

where $\beta = 1/kT$ ($k$: Boltzmann constant), $Z_N$ is the partition function and priori Bernoulli measure $P_N(d\sigma)$. Coarse-graining is carried out by subdividing the lattice into coarse cells and defining variables $\eta(k)$ on each coarse cell to be the total magnetization in the cell. The corresponding renormalization group map, known as the Kadanoff transform [6, 8], is defined by the formula

$$e^{-\beta \bar{H}_M(\eta)} = \int e^{-\beta H_N(\sigma)} P_N(d\sigma|\eta)\,, \tag{1.3}$$

where $\bar{H}_M(\eta)$ is defined as the exactly coarse-grained Hamiltonian and $P_N(d\sigma|\eta)$ is the conditional probability of having a microscopic configuration $\sigma$ given a configuration $\eta$ at the coarse level. Such a Hamiltonian is defined on a coarser level than the microscopic, is an exact equivalent of the microscopic Hamiltonian $H_N$. However, due to the high-dimensional integration, $\bar{H}_M(\eta)$ cannot be easily calculated explicitly and hence used in numerical simulations. The main idea in [14] is to write the exact coarse-grained Hamiltonian $\bar{H}_M(\eta)$ as a perturbation around a first approximation Hamiltonian $\bar{H}^0_M$. The first approximation Hamiltonian $\bar{H}^0_M$, suggested in [10, 11], is defined as,

$$\bar{H}^0_M(\eta) = \int H_N(\sigma) P_N(d\sigma|\eta)\,.$$

Using this first approximation we have from (1.3) that

$$\bar{H}_M(\eta) \;=\; \bar{H}^{(0)}_M(\eta) - \frac{1}{\beta}\log\int e^{-\beta(H_N(\sigma)-\bar{H}^{(0)}_M(\eta))} P_N(d\sigma|\eta)\,. \tag{1.4}$$

It can be shown that $\bar{H}_M(\eta)$ under suitable assumptions can be written as a series expansion around $\bar{H}^{(0)}_M(\eta)$, [14]. Since $\bar{H}_M(\eta), \bar{H}^{(0)}_M(\eta)$ scale as $\mathcal{O}(N)$ hence (1.4)

cannot be expanded using a simple Taylor expansion but instead a cluster expansion is necessary [21] to obtain the following series,

$$\bar{H}_M(\eta) - \bar{H}_M^{(0)}(\eta) = \bar{H}_M^{(1)}(\eta) + \cdots + \bar{H}_M^{(\alpha)}(\eta) + N\mathcal{O}(\epsilon^{\alpha+1})\,,\ p = 2, \ldots \tag{1.5}$$

uniformly in $\eta$, where the correction terms $\bar{H}_M^{(1)}(\eta)$, $\bar{H}_M^{(2)}(\eta)$ etc. can be calculated explicitly, while $\epsilon$ is a parameter depending on the characteristics of the coarse-graining, the potential, and the inverse temperature. Note that the multi-body interactions are given by the $\bar{H}_M^{(2)}(\eta)$ term, see Sect.2.4.

The next step in developing a successful coarse-graining strategy is understanding the error from coarse-graining. For instance, (over-)coarse-graining in polymer systems may yield wrong predictions in the melt structure [1]; similarly wrong predictions on crystallization were also observed in the coarse-graining of complex fluids, [20]. Hence it isimportant to analyze mathematically the error from coarse-graining in order to determine the effectiveness of coarse-graining methods.

The error arising in any attempt to coarse-grain microscopic systems essentially involves the comparison of the coarse-grained probability measures to the projection of the microscopic measure on the coarse variables. One way to the error from coarse-graining is the information lost in terms of microscopic structures and hence a natural way to measure this error is in terms of relative entropy. In information theory the relative entropy $\mathcal{R}(\pi_1 \,|\, \pi_2)$ provides a measure of "information loss" in the approximation of the probability measure $\pi_1$ by or $\pi_2$[4]. The relative entropy of $\pi_1$ with respect to $\pi_2$, for $\pi_1(\sigma)$ and $\pi_2(\sigma)$ two probability measures defined on a common countable state space $\mathcal{S}$, is defined as,

$$\mathcal{R}(\pi_1 \,|\, \pi_2) = \sum_{\sigma \in \mathcal{S}} \pi_1(\sigma) \log \frac{\pi_1(\sigma)}{\pi_2(\sigma)}\,.$$

In our context we use the relative entropy in order to assess the information compression of different coarse-graining schemes, see Scheme 2.1 in Sect.2.4. Furthermore, since we are dealing with extensive systems and compressing local interactions, the errors will also be extensive quantities and it is thus natural to measure the error per unit volume, i.e. in terms of the relative entropy per unit volume. For example, the relative entropy of $\bar{\mu}_{M,\beta}^{(\alpha)}$ the Gibbs measures associated with the Hamiltonian $\bar{H}_M^{(\alpha)}(\eta)$with respect to $\mu_{N,\beta}$ the Gibbs measures associated with the Hamiltonian $\bar{H}_M(\eta)$ (see Scheme 2.2) is given by,

$$\frac{1}{N}\mathcal{R}(\bar{\mu}_{M,\beta}^{(\alpha)} | \mu_{N,\beta} \circ \mathbf{F}^{-1}) \sim \mathcal{O}(\epsilon^{\alpha+1})\,.$$

In this work we first identify the parameter $\epsilon$ corresponding to the coarse-graining, the type of interaction potential, and the inverse temperature, $\beta$. The potentials discussed are power law, Lennard-Jones, Coulomb, Morse and logarithmic which are of relevance in various applied fields. The estimates derived on the coarse-grained methods allow us to compare the relative size and importance of two-body coarse-graine interactions included in $\bar{H}_M^{(0)}$, $\bar{H}_M^{(1)}$ to three-body coarse-graine interactions given by $\bar{H}_M^{(2)}$. of the higher order terms, in particular, $\bar{H}_M^{(1)}$ and $\bar{H}_M^{(2)}$ to emphasize the importance of multi-body interactions that are captured through $\bar{H}_M^{(2)}$. But implementing the higher order coarse-graining scheme which includes multi-body interactions in the case of long-tange potentials can be computationally expensive. Our error estimates

for Scheme 2.1 along with the dependence of the small parameter $\epsilon$ discussed in Sect.3, suggests that we can address this issue of the computational complexity of three-body coarse-graine interactions in two ways: (a) Truncate and compress the three-body terms within a given tolerance (Sect.3.5), or (b) Split the interaction potential $J$ in (1.1) into short-range piece with singularities and a smooth long-range component. Our analysis in Sect.3 shows that if the potential is smooth, long-range and has a long-range decay then the error from two-body coarse-graining using the Hamiltonian $\bar{H}_M^{(0)}$ is small; while for the short-range , possible singularities the three-body corrections are necessary as a 3rd order accurate method Scheme 2.2 maybe needed.

The previous discussion focused mainly on the equilibrium problem. Another aspect of our numerical simulation here focuses on the role of the multi-body coarse-graine interactions on the dynamics. For instance, it was observed in [10] that for long-range interactions the second order coarse-graining scheme was able to capture equilibrium properties like hysteresis accurately. However, when studying dynamical properties e.g. mean times to phase transition, the error from coarse-graining increased substantially especially as level of coarse-graining increased, [13]. The numerical experiments in Sect.5 show that the inclusion of multi-body interactions are critical in accurately reproducing dynamical properties such as rare events, switching times, etc.

The paper is organized as follows: In Sect.2 we present the microscopic model and motivate different coarse-graining schemes. In Sect.3 we focus on error qunatification by identifying the parameter $\epsilon$ in the coarse-graine approximation. We also discuss the relative size and importance of the multi-body interactions using derived estimates for specific potentials. In Sect.4 we give a description of the kinetic Monte-Carlo dynamics and algorithms used for generating the microscopic and the coarse-grained process. In Sect.5 we present simulations with different coarse-graining schemes using the Arrhenius spin-flip dynamics. Finally in Sect.6, we present a discussion on the relation of our schemes to the current coarse-graining schemes in macromolecular systems.

**Acknowledgments:** The research of S.A. was partially supported by NSF-DMS-0413864 and NSF-DMS-0715125. The research of M.A.K. was partially supported by DE-FG02-05ER25702, NSF-DMS-0413864 and NSF-DMS-0715125. The research of P.P. was partially supported by NSF-DMS-0303565. The research or L.R-B. was partially supported by NSF-DMS-0306540.

**2. Equilibrium.** In this section we present the equilibrium model for an Ising-type model. We present the microscopic model by defining the Hamiltonian $H_N(\sigma)$ and the corresponding Gibbs measure $\mu_{N,\beta}$, followed by the coarse-graining procedure and the exact coarse-grained Hamiltonian, $\bar{H}_M(\eta)$. Using formal calculations we motivate the derivation of the first approximation $\bar{H}_M^{(0)}(\eta)$ and a cluster expansion of $\bar{H}_M(\eta)$ around the first approximation $\bar{H}_M^{(0)}(\eta)$. Finally, we present the numerical schemes for coarse-graining with the corresponding error estimates.

**2.1. Microscopic models.** We consider as the physical domain for the system the $d$-dimensional torus $\mathbb{T}_d := [0,1)^d$. The microscopic system consists of a uniform lattice $\Lambda_N := (\frac{1}{n}\mathbb{Z})^d \cap \mathbb{T}_d$. The number of lattice sites $N = n^d$ is fixed, but arbitrary and finite. Although we consider here periodic boundary conditions, but other boundary conditions can be accommodated easily.

The spin (or order parameter) $\sigma(x)$ takes values $\{0,1\}$ at each lattice site $x \in \Lambda_N$. A spin configuration $\sigma = \{\sigma(x)\}_{x\in\Lambda_N}$ is an element of the configuration space $\mathcal{S}_N :=$

$\{0,1\}^{\Lambda_N}$. The energy of the configuration $\sigma$ is given by the Hamiltonian $H_N(\sigma)$, defined in (1.1).

The strength of the potential is measured by $\| J \| \equiv \sum_{x\neq 0} |J(x)|$, i.e., we assume that the two-body potential is summable. A few examples of different potentials are: *Finite-range interactions.* A spin at site $x$ interacts with its neighbors which are at most $L$ lattice points away from $x$. It will be useful to consider the range of the interaction $L$ as a parameter of the model. Then the potential $J(x-y)$ can be taken to have the form

$$J(x-y) = \frac{1}{L^d} V\left(\frac{n}{L}|x-y|\right), \quad x, y \in \Lambda_N \tag{2.1}$$

where the interaction potential is defined through the function $V$ such that, $V : (0,1] \to \mathbb{R}$. The factor $1/L^d$ in (2.1) is a normalization which ensures that the strength of the potential $J$ is essentially independent of $L$ and we have $\| J \| \simeq \int |V(r)| dr$.

*Long-range interactions.* In this case we assume that a spin interacts with all spins i.e. $L = n$ in the above case of finite range interactions and the potential is given by,

$$J(x-y) = \frac{1}{N} V\left(|x-y|\right), \quad x, y \in \Lambda_N$$

*Mixed interactions.* In this case the potential consists of short range and a long range component. The potential looks like,

$$J(x-y) = \frac{1}{S^d} K\left(\frac{n}{S}|x-y|\right) + \frac{1}{L^d} V\left(\frac{n}{L}|x-y|\right), \quad x, y \in \Lambda_N \tag{2.2}$$

where $S$ is the short range interaction length. An interesting case is $K$ and $V$ having different signs, hence $K$ is repulsive and $V$ is attractive,[9].

**2.2. Coarse-grained models.** The coarse-graining procedure consists of three steps that we describe separately.

(a) *Coarse graining of the configuration space.* We partition the torus $\mathbb{T}_d$ into $M = m^d$ cells: For $k = (k_1, \ldots, k_d) \in \mathbb{Z}^d$ with $0 \leq k_i \leq m-1$ we define $C_k \equiv [\frac{k_1}{m}, \frac{k_1+1}{m}) \times \cdots \times [\frac{k_d}{m}, \frac{k_d+1}{m})$ and we have $\mathbb{T}_d = \cup_k C_k$. We identify each cell $C_k$ with a lattice point of the coarse lattice $\bar{\Lambda}_M = (\frac{1}{m}\mathbb{Z})^d \cap \mathbb{T}_d$. Each coarse cell contains $Q = q^d$ points of the microscopic lattice points with $N \equiv n^d = (mq)^d \equiv MQ$. We will refer to $Q$ as the level of coarse-graining ($Q = 1$ corresponds to no coarse-graining). We define a distance function between the coarse cells the $C_k$ and $C_l$,

$$r_{|k-l|} = \frac{1}{m}\left(\sum_{i=1}^{d} (k_i - l_i)^2\right)^{\frac{1}{2}} \quad k,\, l =\in \mathbb{Z}^d \text{ with } 0 \leq k_i, l_i \leq m-1\,.$$

We assign a new spin value $\eta(k)$ for the cell $C_k$ according to the rule

$$\eta(k) := \mathbf{F}(\sigma)(k) = \sum_{x\in C_k} \sigma(x)\,.$$

The spin $\eta(k)$ takes values in $\{0, 1, 2 \ldots, Q\}$ and the configuration space for the coarse-grained system is $\bar{\mathcal{S}}_M \equiv \{0, 1, 2 \ldots, Q\}^{\bar{\Lambda}_M}$.

(b) *Coarse-graining of the prior distribution.* The prior distribution $P_N$ on $\mathcal{S}_N$ induces a new prior distribution on $\bar{\mathcal{S}}_M$ given by $\bar{P}_M(\eta) = P_N(\sigma : \mathbf{F}(\sigma) = \eta)$. The conditional

probability $P_N(d\sigma|\eta)$ plays a crucial role in the definition of a coarse-graine Hamiltonian. Since $\eta(k)$ depends only on the spins $\sigma(x)$, $x \in C_k$, the probability $P_N(d\sigma|\eta)$ factorizes over the coarse cells. We have the following expectations, assuming in each case that all spin sites are different:

$$E_1(\eta) := \mathbb{E}[\sigma(x)|\eta] = \frac{\eta}{Q} \tag{2.3}$$

$$E_2(\eta) := \mathbb{E}[\sigma(x)\sigma(y)|\eta] = \frac{\eta(\eta-1)}{Q(Q-1)} \tag{2.4}$$

$$E_3(\eta) := \mathbb{E}[\sigma(x)\sigma(y)\sigma(z)|\eta] = \frac{\eta(\eta-1)(\eta-2)}{Q(Q-1)(Q-2)} \tag{2.5}$$

$$E_4(\eta) := \mathbb{E}[\sigma(x)\sigma(y)\sigma(z)|\eta] = \frac{\eta(\eta-1)(\eta-2)(\eta-3)}{Q(Q-1)(Q-2)(Q-3)} \tag{2.6}$$

These expectations are used in defining the coarse-graining schemes, which we present in Sect.2.4.

(c) *Coarse-graining of the Hamiltonian.* We want to construct a new Hamiltonian $\bar{H}_M(\eta)$ at the coarse-level. A natural definition of such a Hamiltonian at a coarse level, which we refer to as the *exact* coarse-grained Hamiltonian $\bar{H}_M(\eta)$, is given by,

$$e^{-\beta \bar{H}_M(\eta)} = \mathbb{E}[e^{-\beta H_N}|\eta] = \int e^{-\beta H_N(\sigma)} P_N(d\sigma|\eta)\,. \tag{2.7}$$

Given the Hamiltonian $\bar{H}_M$ we define the corresponding Gibbs measure by

$$\bar{\mu}_{M,\beta}(d\eta) = \frac{1}{\bar{Z}_M} e^{-\beta \bar{H}_M(\eta)} \bar{P}_M(d\eta)\,. \tag{2.8}$$

Even for moderately large values of $N$ the exact computation of $\bar{H}_M(\eta)$ through (2.7) is, in general, impractical. Therefore we want to have a systematic way of calculating explicit approximations of the coarse-grained Hamiltonian $\bar{H}_M$, to any given degree of accuracy. Hence, the main idea is to express $\bar{H}_M$ as a perturbation of an approximation $\bar{H}_M^{(0)}(\eta)$ , i.e. that is we want to write the *exact* coarse-graining $\bar{H}_M$ as,

$$\bar{H}_M - \bar{H}_M^{(0)}(\eta) = \bar{H}_M^{(1)}(\eta) + \cdots + \bar{H}_M^{(p)}(\eta) + N\mathcal{O}(\epsilon^{p+1})$$

where $\epsilon$ is a parameter depending on the characteristics of the coarse-graining that will be precisely identified in Sect.3.

In the next subsection, we try to answer first formally the following questions,

1. How and why do we choose $\bar{H}_M^{(0)}(\eta)$?
2. Once we have the first approximation $\bar{H}_M^{(0)}(\eta)$, how good is the approximation $\bar{H}_M^{(0)}(\eta)$?
3. What is the strategy to get the terms $\bar{H}_M^{(1)}(\eta), \ldots, \bar{H}_M^{(p)}(\eta)$?

**2.3. Formal Calculations.** Suppose we choose $\bar{H}_M^{(0)}(\eta)$, then we can rewrite the exact coarse-graining as a perturbation of $\bar{H}_M^{(0)}(\eta)$ as,

$$e^{-\beta \bar{H}_M(\eta)} = e^{-\beta \bar{H}_M^{(0)}(\eta)} \mathbb{E}[e^{-\beta(H_N(\sigma) - \bar{H}_M^{(0)}(\eta))}|\eta]\,,$$

or equivalently in terms of the Hamiltonian

$$\bar{H}_M(\eta) - \bar{H}_M^{(0)}(\eta) = -\frac{1}{\beta}\log \mathbb{E}[e^{-\beta(H_N(\sigma)-\bar{H}_M^{(0)}(\eta))}|\eta]\,. \tag{2.9}$$

Now if we formally expand the exponential in the second term in (2.9) we obtain,

$$\mathbb{E}[e^{-\beta(H_N(\sigma)-\bar{H}_M^{(0)}(\eta))}|\eta] = 1 + \mathbb{E}[-\beta\Delta H|\eta] + \frac{1}{2}\mathbb{E}[(-\beta\Delta H)^2|\eta] + \dots \tag{2.10}$$

where $\Delta H = H_N(\sigma) - \bar{H}_M^{(0)}(\eta)$. We have from (2.10) that a natural choice for $\bar{H}_M^{(0)}(\eta)$ that is expected to minimize the error, should be such that,

$$\mathbb{E}[\Delta H|\eta] = 0\,. \tag{2.11}$$

Hence the first approximation $\bar{H}_M^{(0)}$ of the coarse-grained Hamiltonian $\bar{H}_M$ is given by the formula

$$\bar{H}_M^{(0)}(\eta) \;\equiv\; \mathbb{E}[H_N|\eta]\,. \tag{2.12}$$

Using (2.3) and (2.4) we thus have,

$$\bar{H}_M^{(0)}(\eta) \;=\; -\frac{1}{2}\sum_k\sum_{l\neq k}\bar{J}(k,l)\eta(k)\eta(l) - \frac{1}{2}\sum_k \bar{J}(0)\eta(k)(\eta(k)-1) + h\sum_k \eta(k)\,.$$

where

$$\begin{aligned}
\bar{J}(k,l) \;&=\; \frac{1}{Q^2}\sum_{x\in C_k, y\in C_l} J(x-y)\,, \quad \text{for } k\neq l,\\
\bar{J}(k,k) \;&=\; \bar{J}(0) = \frac{1}{Q(Q-1)}\sum_{x,y\in C_k, y\neq x} J(x-y)\,, \quad \text{for } k = l.
\end{aligned}$$

Now that we have defined $\bar{H}_M^{(0)}(\eta)$, we proceed to express the *exact* coarse-grained Hamiltonian $\bar{H}_M(\eta)$ as a perturbation of this first approximation. If $\mathbf{F}(\sigma) = \eta$, we can write the difference $H_N(\sigma) - \bar{H}_M^{(0)}(\eta)$ as,

$$\begin{aligned}
H_N(\sigma) - \bar{H}_M^{(0)}(\eta) &= \sum_k\sum_{l\neq k}\Delta_{kl}J(\sigma)\,, \quad \text{where}\\
\Delta_{kl}J(\sigma) &:= -\frac{1}{2}\sum_{\substack{x\in C_k\\ y\in C_l, y\neq x}} (J(x-y) - \bar{J}(k,l))\sigma(x)\sigma(y)\,.
\end{aligned} \tag{2.13}$$

Note that the above difference is an extensive quantity and hence is not necessarily small, it is in fact of order $N\epsilon$.The expectation in the second term in (2.10) becomes,

$$\mathbb{E}[e^{-\beta(H_N(\sigma)-\bar{H}_M^{(0)}(\eta))}|\eta] = \mathbb{E}[\,e^{\sum_{k,l}-\beta\Delta_{kl}J(\sigma)}|\eta] = \mathbb{E}[\prod_{k,\,l} e^{-\beta\Delta_{kl}J(\sigma)}|\eta] \tag{2.14}$$

Only formally, Taylor expansion of the logarithm enable us to write the right hand term of (2.9) as,

$$\begin{aligned}
\frac{1}{\beta}\log \mathbb{E}[e^{-\beta(H_N(\sigma)-\bar{H}_M^{(0)}(\eta))}|\eta] \;&=\; \frac{1}{\beta}\log\int \prod_{k,\,l} e^{-\beta\Delta_{kl}J(\sigma)}P_N(d\sigma|\eta)\\
&=\; \frac{1}{\beta}\log\int\prod_{k,\,l}(1+\sum_{p=1}^{\infty}\frac{1}{p!}(-\beta\Delta_{kl}J(\sigma))^p)\prod_k\tilde{\rho}_k(d\sigma)\\
&:= \bar{H}_M^{(1)}(\eta) + \bar{H}_M^{(2)}(\eta) + \dots
\end{aligned} \tag{2.15}$$

Cluster expansions are tools which allow expansion of such quantities rigourously in convergent power series using the independence properties of product measures. The crucial fact here is that the conditional measure $P_N(d\sigma|\eta)$ factorizes over the coarse cells. In the next section we present the coarse-graining schemes derived using cluster expansions, for a detailed theoretical description we refer to [14].

**2.4. Coarse-graining schemes.** Before we proceed to the statement of numerical schemes we first introduce some notation as suggested by the calculations in Sect.2.3. To calculate the higher order corrections requires the expansion of the terms in (2.15) which involve the following quantities that can viewed as spatial correlations of the potential $J$,

$$j^1_{kl} := \sum_{\substack{x\in C_k\\ y\in C_l}} (J(x-y)-\bar J(k,l))^2 \tag{2.16}$$

$$j^2_{kl} := \sum_{\substack{x\in C_k\\ y,y'\in C_l}} (J(x-y)-\bar J(k,l))(J(x-y')-\bar J(k,l)) \tag{2.17}$$

$$j^2_{k_1k_2k_3} := \sum_{\substack{x\in C_{k_1}\\ y\in C_{k_2},z\in C_{k_3}}} (J(x-y)-\bar J(k_1,k_2))(J(y-z)-\bar J(k_2,k_3)) \tag{2.18}$$

If $k_1=k_2$ then we also impose that for $x,y\in C_{k_1}$ we have $y\neq x$. Note also that these quantities have various symmetries, for example, $j^2_{lk}=j^2_{kl}$ or $j^1_{kl}=\tilde j^1_{k-l}=\tilde j^1_{l-k}$ for some function $\tilde j^1$ and similarly $j^2_{kl}$ depends only on $|k-l|$, moreover $j^2_{k_1k_2k_3}=\tilde j^2_{k_1-k_2,k_3-k_2}$.

As suggested by (2.9), we can view $\epsilon$ as a parameter that is proportional to $|H_N(\sigma)-\bar H^{(0)}_M(\eta)|$ and also dependent on the temperature $\beta$,

$$\epsilon \equiv \frac{\beta}{N}\sup_\sigma |H_N(\sigma)-\bar H^{(0)}_M(\eta)|\,. \tag{2.19}$$

Here we present only two schemes, we call them 2nd and 3rd-order schemes as they are 2nd and 3rd-order accurate in relative entropy.

SCHEME 2.1 (2nd order two-body CG interactions). *The 2nd order coarse-graining algorithm has the following characteristics*

1. *The Hamiltonian: $\bar H^{(0)}_M$, given by (2.12) written as,*

$$\bar H^{(0)}_M(\eta)=\sum_{k\neq l}\Lambda^{(0)}_2(k,l;\,,\eta(k),\eta(l))+\sum_k\Lambda^{(0)}_1(k;\,\eta(k))$$

*where,*

$$\Lambda^{(0)}_2(k,l;\,\eta(k),\eta(l)) = -\frac{1}{2}\bar J(k,l)\eta(k)\eta(l)$$
$$\Lambda^{(0)}_1(k;\,\eta(k)) = -\frac{1}{2}\bar J(0)\eta(k)(\eta(k)-1)+h\eta(k)$$

2. *The Gibbs measure: $\bar\mu^{(0)}_{M,\beta}$, given by $\bar\mu^{(0)}_{M,\beta}(d\eta)=\frac{1}{\bar Z^{(2)}_M}e^{-\bar H^{(0)}_M}\bar P_M(d\eta)$.*
3. *The Relative entropy error*

$$N^{-1}\mathcal{R}(\bar\mu^{(0)}_{M,\beta}|\mu_{N,\beta}\circ\mathbf{F}^{-1})\sim\mathcal{O}(\epsilon^2)\,.$$

SCHEME 2.2 (3rd order multi-body CG interactions). *The 3rd order coarse-graining algorithm has the following characteristics*

1. *The Hamiltonian:* $\bar{H}_M^{(0)} + \bar{H}_M^{(1)} + \bar{H}_M^{(2)}$ *,where the corrections are*

$$\bar{H}_M^{(1)}(\eta) = \sum_{k<l} \Lambda_2^{(1)}(k,l;\,\eta(k),\eta(l)) + \sum_k \Lambda_1^{(1)}(k;\,\eta(k))$$

*where,*

$$\begin{aligned}\Lambda_2^{(1)}(k,l;\,\eta(k),\eta(l)) = \frac{\beta}{2}\big(&j_{kl}^1\,[E_2(\eta(k))E_2(\eta(l)) - E_1(\eta(k))E_2(\eta(l))\\ &- E_2(\eta(k))E_2(\eta(l)) + E_1(\eta(k))E_1(\eta(l))]\\ &+ j_{kl}^2\,[-2E_2(\eta(k))E_2(\eta(l)) + E_2(\eta(k))E_1(\eta(l))\\ &+ E_1(\eta(k))E_2(\eta(l))]\,\big)\\ \Lambda_1^{(1)}(k;\,\eta(k)) = \frac{\beta}{8}\big(&4j_{kk}^2\,[-E_4(\eta(k)) + E_3(\eta(k)]\\ &+2j_{kk}^1\,[E_4(\eta(k)) + E_2(\eta(k)) - 2E_3(\eta(k))]\big)\end{aligned}$$

*and*

$$\bar{H}_M^{(2)}(\eta) = \sum_{k\neq l} \Lambda_2^{(2)}(k,l,k;\eta(k),\eta(l),\eta(k)) + \sum_{k<l<m} \Lambda_3^{(2)}(k,l,m;\eta(k),\eta(l),\eta(m))$$

*where,*

$$\begin{aligned}\Lambda_2^{(2)}(k,l,k;\,\eta(k),\eta(l),\eta(k)) = -\frac{\beta}{2}\big(&j_{kkl}^2\,[-E_3(\eta(k))E_1(\eta(l)) + E_2(\eta(k))E_1(\eta(l)) +\\ &E_1(\eta(k))E_2(\eta(l)) - E_3(\eta(l))E_1(\eta(k))\,]\big)\end{aligned}$$

$$\begin{aligned}\Lambda_3^{(2)}(k,l,m;\,\eta(k),\eta(l),\eta(m)) = \beta\big(&j_{klm}^2\,[E_1(\eta(k))E_1(\eta(m))(1 - E_2(\eta(l)))]\\ &+j_{lmk}^2\,[E_1(\eta(k))E_1(\eta(l))(1 - E_2(\eta(m)))]\\ &+ j_{mkl}^2\,[E_1(\eta(m))E_1(\eta(l))(1 - E_2(\eta(k)))]\big)\end{aligned}$$

*The terms* $E_i$ *are defined in (2.3-2.6) and the quantities* $j_{kl}^1, j_{kl}^2, j_{k_1k_2k_3}^2$ *are defined in (2.16-2.18).*

2. *The Gibbs measure* $\bar{\mu}_{M,\beta}^{(2)}(d\eta) = \frac{1}{\bar{Z}_M^{(2)}} e^{-(\bar{H}_M^{(0)} + \bar{H}_M^{(1)} + \bar{H}_M^{(2)})} \bar{P}_M(d\eta)$.
3. *The Relative entropy error*

$$N^{-1}\mathcal{R}(\bar{\mu}_{M,\beta}^{(2)} | \mu_{N,\beta} \circ \mathbf{F}^{-1}) \sim \mathcal{O}(\epsilon^3)\,.$$

Note that the way we defined the schemes $\bar{H}_M^{(0)}(\eta)$ consists of only two-body interactions as does $\bar{H}_M^{(1)}(\eta)$ where as $\bar{H}_M^{(2)}(\eta)$ consists of three-body interactions. Note $\Lambda_2^{(2)}$ is essentially three-body interaction even though it involves only two coarse cells, this follows from the graphs in the polymer model used for cluster expansion [14].

REMARK 1.

1. We note that in information theory the relative entropy $\mathcal{R}$ provides a measure of "information distance" of two probability measures. In our context we use

the relative entropy estimates in order to assess the information compression of different coarse-graining schemes. According to how many correction terms are included in the expansion corresponding to different truncation levels, such as Scheme 2.1 and Scheme 2.2 in Sect.2.4, we quantify the amount of information loss when the measures are compared at the same level of coarse-graining.

2. Note that the multi-body interactions given by $\bar{H}_M^{(2)}(\eta)$ in Scheme 2.2 are also temperature dependent and hence they are expected to be more important in low temperature regime rather than in high temperature regimes. We show in the next section the precise dependence of the correction terms on temperature. Temperature dependence of the corrections has been seen in coarse-graining of polymer chains (see Sect.6), where most of the schemes do not include the multi-body interactions.

The multi-body interactions such as the three-body interactions in Scheme 2.2, from a computational point of view, can be expensive. Hence it is important to understand where the multi-body interactions, for instance we observe that when coarse-graining smooth potentials with a decay the Scheme 2.1 is an accurate approximation and does not require including the multi-body interactions. We also require to identify strategies like truncating the multi-body interactions, splitting the potentials to make multi-body interactions computationally feasible.

**3. Error quantification and Multi-body interactions.** In this section we first focus on analyzing the dependence of the coarse-graining error on the detailed characteristics of the interaction potential $J$.

Using the estimates for specific potentials we estimate the size of the multi-body interactions and compare them with the two-body interactions. To address the computational complexity associated with implementing the multi-body interactions we use the error estimates to show that the multi-body interactions can be truncated to a given tolerance or if the potential has a smooth long range decay then it can split the potential appropriately and use different coarse-graining schemes on different pieces.

We first start by looking at the error as the sum of the error from short ranged interactions between coarse cells and the error from long range interactions of the coarse cells. Considering the coarse-graining error in this way allows us to control and estimate exactly the error from each piece of the potential based on its behavior.

To do this we associate a coarse distance $r_c$ with a given potential based on which we classify the interactions as either being short range or long range. Once we have $r_c$ the error can be broken into two pieces as given by the following trivial lemma,

LEMMA 3.1. *If* $\mathbf{F}(\sigma) = \eta$, *we have,*

$$\epsilon = \frac{\beta}{N}\left|H_N(\sigma) - \bar{H}_M^{(0)}(\eta)\right| \leq \frac{\beta}{N}\sum_k \left[\sum_{\{l\,:\,r_{|k-l|}\leq r_c\}} \mathrm{D}_{kl} + \sum_{\{l\,:\,r_{|k-l|}> r_c\}} \mathrm{D}_{kl}\right]$$

where,

$$E_{kl}(x-y) := J(x-y) - \bar{J}(k,l)\,, \quad x \in C_k, y \in C_l\,,$$

which measures the variation of the potential $J(x-y)$ over a cell. We also define,

$$\mathrm{D}_{kl} := \sum_{x\in C_k\,, y\in C_l} |E_{kl}(x,y)|\,, \quad x \neq y \text{ if } k = l$$

which measures the total variation of the potential $J(x-y)$.
PROOF: We have that,

$$\begin{aligned}\frac{\beta}{N}|H_N(\sigma)-\bar{H}_M^{(0)}(\eta)| \le \frac{\beta}{N}\sum_k \Bigg[ &\sum_{\{l\,:\,r_{|k-l|}\le r_c\}} \left( \sum_{\substack{x\in C_k \\ y\in C_l, y\neq x}} |J(x,y)-\bar{J}(k,l)| \right) \\ &+ \sum_{\{l\,:\,r_{|k-l|}> r_c\}} \left( \sum_{\substack{x\in C_k \\ y\in C_l, y\neq x}} |J(x,y)-\bar{J}(k,l)| \right) \Bigg] \\ := \epsilon_s + \epsilon_l\end{aligned}$$

The term $\epsilon_s$ is the error from coarse-graining the short range interactions while the term $\epsilon_l$ is the error from coarse-graining the long range interactions.

Now we present a few examples for potential which are of relevance to various applied fields and identify the error the parameter $\epsilon$ in (2.19) as suggested by Lemma 3.1, the details are rather straight forward are presented in AppendixA.

**3.1. Piecewise constant potential.** Before we proceed to study general potentials, we analyze piecewise constant potential which is widely used in simulations. Note that even though we present this discussion of the piecewise constant in one dimension, it can be extended to higher dimensions. Suppose that $V(r)=\frac{J_0}{2}$ for $|r|\le 1$, zero otherwise and $J$ is given by (2.1) with interaction radius $L$, i.e. $J(x-y)=\frac{J_0}{2L}$ when $|x-y|\le L$. Assume that the coarse-graining level is $q$ and the coarse length of the interaction $\bar{L}=\dfrac{L}{q}\in\mathbb{Z}$, then it follows by simple counting, that the parameter $\epsilon$ is given by,

$$\epsilon \equiv \beta\frac{1}{q}\left(\frac{J_0}{4L}(q^2-1)+\frac{J_0}{L}\left(\frac{2q-1}{q}+\frac{q-2}{q^2}\right)\right). \tag{3.1}$$

The $\epsilon$ in (3.1) implies that Scheme 2.1 is expected to work well when $\frac{q}{L} << 1$ otherwise Scheme 2.2 is more suitable. This has been studied in [14] and here.

**3.2. Power law type potential.** Assume that $J$ is given by (2.1) and $V\in C^1(0,\infty)$ satisfies

$$|V(r)|\le \frac{K}{r^\alpha}, \quad |V'(r)|\le \frac{K\alpha}{r^{\alpha+1}}, \quad \text{for } r>r_c; \tag{3.2}$$

Then we have,

1. For all $k,l$ such that $r_{|k-l|}>r_c$,

$$|\bar{J}(k,l)|\le \frac{K}{N}\frac{1}{(r_{|k-l|})^\alpha} \tag{3.3}$$

2. For all $k,l$ such that $r_{|k-l|}>r_c$, if $x\in C_k$ and $y\in C_l$

$$|J(x,y)-\bar{J}(k,l)|\le \frac{2K\alpha\sqrt{d}}{q^d m^{d+1}}\ \frac{1}{(r_{|k-l|})^{\alpha+1}} \tag{3.4}$$

Based on the above estimates the parameter $\epsilon$ is given by,

$$\begin{aligned}\epsilon &\equiv \beta \frac{1}{q^d}\left(\sum_{\{l\,:\,r_l\le r_c\}} \mathrm{D}_{r_l}\right) + \beta\,\frac{2K\alpha\sqrt{d}}{m}\frac{2\pi^{\frac{d}{2}}}{\Gamma(\frac{d}{2})}\left[\frac{1-(r_c)^{(d-1-\alpha)}}{(d-1-\alpha)}\right] \\ &:= \epsilon_s + \epsilon_l\,.\end{aligned} \tag{3.5}$$

where $\epsilon_s$ and $\epsilon_l$ represent the error made by coarse-graining the short range interactions and long range interactions respectively. This estimate suggests if the coarse-graine grid (namely $m$ is large enough ) is such that $\epsilon_l$ is small and also the potential is such that $\epsilon_s$ is small then Scheme 2.1 may perform well, see Fig.5.2. The estimate also suggests the potential splitting method when the potentials have smooth long-range decay, see Sect.3.6.

**3.3. Potentials with integrable singularity.** Assume $V$ satisfies$r^{d-1}V'(r) \in L^1(0,\infty)$ such potentials includes Coulomb interactions where the interactions are inversely proportional to the distance in $\mathbb{R}^3$ [21] and 2-D turbulence where the interactions are proportional to the logarithm of the distance between two interacting sites[23].

Assume that $J$ is given by (2.1),(**??**), $V(r) \in C^1(0,\infty)$ and $r^{d-1}V'(r) \in L^1(0,\infty)$,

1. If $x \in C_k$ and $y \in C_l$, we have

$$|J(x,y) - \bar{J}(k,l)| \le \frac{1}{N}\|r^{d-1}V'\|_{L^1(r_{kl}-\frac{\sqrt{d}}{m},r_{kl}+\frac{\sqrt{d}}{m})} \tag{3.6}$$

The parameter $\epsilon$ is given by,

$$\epsilon \equiv \beta\frac{4K\sqrt{d}\,\pi^{d/2}}{m}\|z^{d-1}V'(z)\|_{L^1}. \tag{3.7}$$

Hence $\epsilon$ is small provided we have suitable conditions on the coarse-graine grid and the radial norm of $V'$. In which case just Scheme 2.1 is expected to perform well.

**3.4. Relative size of the corrections.** We have seen that effectiveness of the Scheme 2.1 depends on the properties of the potential $J(x,y)$ and the first approximation $\bar{J}(k,l)$. To construct the higher order corrections we see that the size of $E_{kl}(x-y)$ is an important quantity which determines which of the two schemes presented in Sect.2.4 is appropriate. Since the terms $E_i(\alpha)$ are of order one, the size of the higher order terms is determined by the size of $j^1_{kl}, j^2_{kl}$ and $j^2_{klm}$. As pointed out earlier, $\bar{H}^{(0)}_M(\eta)$, $\bar{H}^{(1)}_M(\eta)$ include only the two body interactions where as $\bar{H}^{(2)}_M(\eta)$includes three-body interactions. Based on Sect.3.2 we derive the following estimates for the power law-type potentials,

$$\begin{aligned}
&j^1_{kl} \sim \mathrm{D}^2_{kl} && \text{for } k,l \text{ such that } r_{|k-l|} \le r_c \\
&j^2_{kl} \sim Q\,\mathrm{D}^2_{kl} && \text{for } k,l \text{ such that } r_{|k-l|} \le r_c \\
&j^1_{kl} \sim \left(\frac{2K\alpha\sqrt{d}}{m^{d+1}}\frac{1}{(r_{|k-l|})^{\alpha+1}}\right)^2 && \text{for } k,l \text{ such that } r_{|k-l|} > r_c \\
&j^2_{kl} \sim Q\left(\frac{2K\alpha\sqrt{d}}{m^{d+1}}\frac{1}{(r_{|k-l|})^{\alpha+1}}\right)^2 && \text{for } k,l \text{ such that } r_{|k-l|} > r_c \\
&j^2_{klm} \sim Q\,\mathrm{D}_{kl}\mathrm{D}_{lm} && \text{for } k,l \text{ such that } r_{|k-l|} \le r_c\,, r_{|l-m|} \le r_c
\end{aligned} \tag{3.8}$$

$$
\begin{aligned}
j^2_{klm} &\sim Q\,\mathrm{D}_{kl}\left(\frac{2K\alpha\sqrt{d}}{m^{d+1}}\right)\left(\frac{1}{r_{|l-m|}}\right)^{\alpha+1} && \text{for } k,l \text{ such that } r_{|k-l|}\le r_c\,, r_{|l-m|}> r_c\\
j^2_{klm} &\sim Q\left(\frac{2K\alpha\sqrt{d}}{m^{d+1}}\right)^2\left(\frac{1}{r_{|k-l|}r_{|l-m|}}\right)^{\alpha+1} && \text{for } k,l \text{ such that } r_{|k-l|}> r_c\,, r_{|l-m|}> r_c
\end{aligned}
\tag{3.9}
$$

The estimates in (3.9) show that the $j^2_{kl}$ terms in $\bar{H}^{(1)}_M$ and $j^2_{klm}$ terms in $\bar{H}^{(2)}_M$are of the same order. Using the estimates in (3.9) and comparing $\bar{H}^{(1)}_M$ and $\bar{H}^{(2)}_M$ for a fixed $k$, $l$ we have that,

$$
\begin{aligned}
\bar{H}^1_M &\sim 2D^2_{00} + 4Q\left(\frac{2K\alpha\sqrt{d}}{m^{d+1}}\right)^2\left(\frac{1}{(r_{|k-l|})^{\alpha+1}}\right)^2\\
\bar{H}^2_M &\sim QD_{00}\left(\frac{2K\alpha\sqrt{d}}{m^{d+1}}\right)\left(\frac{1}{r_{|k-l|}}\right)^{\alpha+1}\\
&\quad + 2Q\left(\frac{2K\alpha\sqrt{d}}{m^{d+1}}\right)\left(\frac{1}{r_{|k-l|}}\right)^{\alpha+1}\left[\sum_{0<r_{lm}\le r_c} D_{lm} + \sum_{r_{lm}\ge r_c}\left(\frac{2K\alpha\sqrt{d}}{m^{d+1}}\right)\left(\frac{1}{r_{|l-m|}}\right)^{\alpha+1}\right]\\
&\quad + 2Q\left(\frac{2K\alpha\sqrt{d}}{m^{d+1}}\right)\left(\frac{1}{r_{|k-m|}}\right)^{\alpha+1}\left[\sum_{0<r_{lm}\le r_c} D_{lm} + \sum_{r_{lm}\ge r_c}\left(\frac{2K\alpha\sqrt{d}}{m^{d+1}}\right)\left(\frac{1}{r_{|l-m|}}\right)^{\alpha+1}\right]\\
&\quad + 2Q\left(\frac{2K\alpha\sqrt{d}}{m^{d+1}}\right)^2\left(\frac{1}{r_{|k-m|}}\right)^{\alpha+1}\left(\frac{1}{r_{|k-l|}}\right)^{\alpha+1}
\end{aligned}
\tag{3.10}
$$

The estimates in (3.10) imply that the three body interactions in $\bar{H}^{(2)}_M$ are at least of the same order as $\bar{H}^{(1)}_M$. The whole idea of these estimates is to convey the fact that it is important to include three body interactions (namely $\bar{H}^2_M$) for improving upon the coarse-graining scheme using $\bar{H}^{(0)}_M$. We will further discuss the importance of the $\bar{H}^{(2)}_M$ in Sect.6 in the context of coarse-graining of polymer chains. We next to look to address the computational complexity associated with implementing the multi-body interactions.

**3.5. Truncations.** From a computational point of view calculating the three body corrections, i.e. $\bar{H}^{(2)}_M(\eta)$ can be quite expensive depending on the size of the matrix $j^2_{klm}$. Based on the estimates from Sect.3.2 we can further compress the corrections, by discarding the interactions when $k$ and $l$ are sufficiently far apart, i.e. restricting the three-body interactions at any given coarse location. Since we know exactly the order of the individual terms in the corrections we can control the error within a given tolerance when we truncate the corrections. For instance, for the power law-type potential the error from truncating the corrections after a coarse distance of $\bar{L}_1$ is $\mathcal{O}\left(\beta Q\left(\frac{2\alpha\sqrt{d}K}{m\bar{L}_1^{\alpha+1}}\right)^2\right)$.

We define the total error as the error from Scheme 2.2 and the error from trun-

cating the the corrections is given by,

$$\begin{aligned} Tot.error &:= \frac{\beta}{N}\left(\bar{H}_M(\eta) - (\bar{H}_M^{(0)}(\eta) + \bar{H}_M^{(1)}(\eta) + \tilde{H}_M^{(2)}(\eta)\right) \\ &\equiv \mathcal{O}(\epsilon^3) + \mathcal{O}\left(\beta Q\left(\frac{2\alpha\sqrt{d}K}{m\bar{L}_1^{\alpha+1}}\right)^2\right) \end{aligned} \tag{3.11}$$

where $\tilde{H}_M^{(2)}(\eta)$ is the 3-body term obtained by truncating $\bar{H}_M^{(2)}(\eta)$.

**3.6. Potential-Splitting.** As suggested by the example and the discussion in Sect.3 another approach to further increase the computational efficiency of the schemes presented in Sect.2.4 is to split the potential by identifying the size of the error due to the coarse-graining of the potential. There the error estimates suggest a natural way is to split the potential in a short range piece with possible singularities and a smooth long range decaying component,

$$J(x,y) = J_s(x,y) + J_l(x,y)$$

where $J_s(x,y) = J(x,y)\,\mathbf{I}_{[0,r_c]}(|x-y|)$, $J_l(x,y) = J(x,y)\,\mathbf{I}_{(r_c,\infty)}(|x-y|)$ and $r_c$ is an adjustable radius. Thus the computational expense in implementing higher order coarse-graining schemes (Scheme 2.2) can be decreased by implementing a higher order coarse-graining scheme for the short range piece $J_s(x,y)$ alone and implementing a 2nd-order coarse-graining scheme (Scheme 2.1) for the long range piece $J_l(x,y)$. The latter is sufficient provided that $m$ is large enough in (3.5). Splitting the potential is an efficient way of handling the multi-body terms which involve the $j_{klm}^2$ terms especially when the interactions are long-range in which case the calculating $j_{klm}^2$ for all $k,l,m$ may become intractable unless we can substantially truncate the matrix as discussed in Section 3.5. We can also use this approach when the interactions are of *mixed interactions* type as given by (2.2), where the potential is already broken into short range and long range pieces. We refer to the example considered in Sect.3.2 as well as in the simulations depicted in Fig.5.4.

**4. Coarse-grained stochastic dynamics.** In this section we extend our analysis to construct efficient and accurate coarse-graining methods for the approximation of not only the equilibrium invariant measure $\mu_{N,\beta}$ but also for the approximation of the measure on the path space. We start by a brief description of the microscopic and the coarse-grained lattice dynamics.

**4.1. Microscopic Monte Carlo algorithms.** The sampling algorithm for the microscopic lattice system is given in terms a continuous-time jump Markov process $\{\sigma_t\}_{t\geq 0}$. The generator of this stochastic process $\mathcal{L}_N$ is given by,

$$(\mathcal{L}_N f)(\sigma) = \sum_{x\in\Lambda_N} c(x,\sigma)\left(f(\sigma^x) - f(\sigma)\right). \tag{4.1}$$

for bounded test function $f \in L^\infty(\mathcal{S}_N)$. Here $c(x,\sigma)$ denotes the rate of the process and $\sigma^x$ signifies the configuration after a flip at $x$.

In general for sampling the equilibrium Gibbs measure a wide class of Metropolis-type algorithms are available [10, 11].The Kinetic Monte Carlo(KMC) methods [3] are such methods which are also used to simulate non-equilibrium processes. The dynamics in such a case is known as *Arrhenius dynamics*. The rates are usually

derived from transition state theory or obtained from molecular dynamics simulations. The Arrhenius spin flip rate is defined as follows

$$c(x,\sigma) = d_0\sigma(x) + d_0(1-\sigma(x))e^{-\beta U(x,\sigma)} \tag{4.2}$$

where $U(x,\sigma)$ is the potential which is given by,

$$U(x,\sigma) = \sum_{y\in\Lambda_N\, y\neq x} J(x-y)\sigma(y)\,. \tag{4.3}$$

It can be easily verified that the Arrhenius rate defined in (4.2) satisfies the detailed balance condition given by,

$$c(x,\sigma)e^{-\beta H(\sigma)} = c(x,\sigma^x)e^{-\beta H(\sigma^x)}\,. \tag{4.4}$$

**4.2. Coarse-grained Monte Carlo algorithms.** Given the Markov process $(\{\sigma_t\}_{t\geq 0},\ \mathcal{L})$ with the generator $\mathcal{L}$ we obtain a coarse-grained process $\{\mathbf{F}(\sigma_t)\}_{t\geq 0}$. The fact that the process $\{\mathbf{F}(\sigma_t)\}_{t\geq 0}$, in general, is not a Markov process poses a significant difficulty mathematically and computationally in studying this process. Hence we derive an approximating coarse-grained Markov process $(\{\eta_t\}_{t\geq 0}, \bar{\mathcal{L}}^c)$ which can be easily implemented once its generator is given explicitly.

For the purpose of sampling the coarse-grained Gibbs measure given by $\bar{\mu}^{(0)}_{M,\beta}(\eta)$ we will consider a Markov jump process with the generator

$$\bar{\mathcal{L}}^c g(\eta) = \sum_{k\in\bar{\Lambda}_M} \bar{c}_b(k,\eta)\left[g(\eta+\delta_k)-g(\eta)\right] + \sum_{k\in\bar{\Lambda}_M} \bar{c}_d(k,\eta)\left[g(\eta-\delta_k)-g(\eta)\right]\,. \tag{4.5}$$

where the rates $\bar{c}_b(k,\eta), \bar{c}_d(k,\eta)$ correspond to the adding a particle ("birth") and removing a particle ("death") from the coarse cell.

In case of non-equilibrium dynamics like the *Arrhenius dynamics* the strategy is to derive the rates $\bar{c}_b(k,\eta), \bar{c}_d(k,\eta)$ which have the same form as the microscopic rates for *Arrhenius dynamics* given by (4.2). Deriving the rates in this way allows us not only to approximate the measure $\mu_{N,\beta}(\sigma)$ but also gives an approximation of the measure on the path space. The approximate rates are given by, see [10, 11],

$$\bar{c}_a(k,\eta) = d_0(q-\eta(k))\,, \qquad \bar{c}_d(k,\eta) = d_0\eta(k)e^{-\beta(\bar{U}^{(0)}(k,\eta)} \tag{4.6}$$

where the new interaction potential $\bar{U}^{(0)}(\eta)$ represents an approximations of the original interaction potential $U(\sigma)$ and is given by:

$$\bar{U}^{(0)}(k,\eta) = \sum_{\substack{l\in\bar{\Lambda}_M\\ l\neq k}} \bar{J}(l,k)\eta(l) + \bar{J}(0,0)(\eta(k)-1)\,. \tag{4.7}$$

We note that by definition $\bar{U}^{(0)}(k,\eta)$ satisfies the following conditons,

$$\bar{U}^{(0)}(k,\eta) = \bar{H}^{(0)}(\eta) - \bar{H}^{(0)}(\eta-\delta_k)$$

which as shown in [10] is sufficient for the detailed balance (4.4) for the coarse-grained rates.

In [16], rigorous analysis of CGMC algorithms as approximations of MC in *non-equilibrium* using the concept of *relative entropy* as a quantitative measure for the

*loss of information* during coarse-graining. The following estimate between the time dependent probability, $\mu_{m,q,\beta}(t)$, and the exact projection on the coarse variables of the microscopic probability, $\mu_{N,\beta} \circ \mathbf{F}^{-1}(t)$ was obtained:

$$\mathcal{R}(\mu_{m,q,\beta}(t)|\mu_{N,\beta} \circ \mathbf{F}^{-1}(t)) = \mathcal{O}_T(\epsilon), \quad t \in [0,T] \tag{4.8}$$

REMARK 2. Note that the estimate presented in [16] is only $\mathcal{O}_T(\epsilon)$ but we expect error estimate of the order $\mathcal{O}_T(\epsilon^2)$ using the same analysis as in [16] and taking into account the cancellations due to (2.11) as was done in [13] for weak topology estimates. We also refer to [15] for coarse-graine Langevin type approximation to KMC.

*Higher Order algorithms.* For sampling the Gibbs measure $\bar{\mu}^{(\alpha)}_{M,\beta}(\eta)$ corresponding to $\bar{H}^{(\alpha)}_M$ we consider a Markov jump process with higher order coarse-grain rates $\bar{c}^{(\alpha)}_a(k,\eta)$, $\bar{c}^{(\alpha)}_d(k,\eta)$. For the *Arrhenius dynammics* we define the new coarse-grained rates as,

$$\bar{c}^{(\alpha)}_a(k,\eta) = d_0(q-\eta(k))\,, \qquad \bar{c}^{(\alpha)}_d(k,\eta) = d_0\eta(k)e^{-\beta(\bar{U}^{(0)}(\eta)+\ldots+U^{(\alpha)}(\eta))}\,,$$

where $\alpha = 1, 2, \ldots$. The new interaction potential $\bar{U}^{(0)}(\eta) + \ldots + U^{(\alpha)}(\eta))$ represents the higher order approximation of the original interaction $U(\sigma)$. In order to satisfy the detailed balance condition (4.4) for the higher-order coarse-grained Gibbs measure we define higher order coarse potentials as,

$$\bar{U}^{(\alpha)}(\eta) := \bar{H}^{(\alpha)}(\eta) - \bar{H}^{(\alpha)}(\eta - \delta_k)\,, \tag{4.9}$$

where $\alpha = 0, 1, \ldots$.

It is important to realise that just as in (4.7) calculating $\bar{U}^{(\alpha)}(\eta)$ involves a local difference and does not require to calculate the complete Hamiltonian. Specifically for Scheme 2.2 the higher-order potentials are given by:

$$\begin{aligned}
\bar{U}^{(1)}(k,\eta) = & \sum_{\substack{l\in\bar{\Lambda}_M \\ l\neq k}} \Big[\Lambda^{(1)}_2(k,l;\,\eta_k,\eta_l) - \Lambda^{(1)}_2(k,l;\,\eta_k-1,\eta_l)\Big] \\
& + \Lambda^{(1)}_1(k;\,\eta_k) - \Lambda^{(1)}_1(k;\,\eta_k-1) \\
\bar{U}^{(2)}(k,\eta) = & \sum_{\substack{l\in\bar{\Lambda}_M \\ l\neq k}} \Big[\Lambda^{(2)}_2(k,l,k;\,\eta_k,\eta_l,\eta_k) - \Lambda^{(2)}_2(k,l,k;\,\eta_k-1,\eta_l,\eta_k-1)\Big] \\
& + \sum_{l<m} \Big[\Lambda^{(2)}_3(k,l,m;\,\eta_k,\eta_l,\eta_m) - \Lambda^{(2)}_3(k,l,m;\,\eta_k-1,\eta_l,\eta_m)\Big]
\end{aligned} \tag{4.10}$$

Note that these calculations can also be simplified by truncating as in Sect.3.5 or by splitting the potential as in Sect.3.6.

The analysis in [16], suggests that the estimate between the time dependent probability, $\mu^{(\alpha)}_{m,q,\beta}(t)$, and the exact projection on the coarse variables of the microscopic probability, $\mu_{N,\beta} \circ \mathbf{F}^{-1}(t)$ may be of higher order, e.g.

$$\mathcal{R}(\mu^{(\alpha)}_{m,q,\beta}(t)|\mu_{N,\beta} \circ \mathbf{F}^{-1}(t)) = \mathcal{O}_T(\epsilon^{\alpha+1}), \quad t \in [0,T] \tag{4.11}$$

However we do not have a proof of this conjecture at this point. Clearly the dynamics simulations in Fig.5.7, 5.8, 5.9 and the Table 5.1 suggest a higher order accuracy than the dynamics based on the (4.6).

**5. Computational algorithms and numerical experiments.** The 2nd-order approximation for the coarse-grained algorithm as described in Scheme 2.1 has been extensively studied in the previous works, see, e.g., [11, 10, 13], where it has been demonstrated that it performs well in high temperature regimes or when long-range interactions are involved (even in low temperature regimes). In coarse-grained Monte Carlo (CGMC) simulations for lattice systems, hysteresis and critical behavior are also not captured properly for short and intermediate range potentials, [10], but using the 3rd order coarse-graining scheme the error was substantially reduced,[14, 12]. In the numerical simulations presented we implement the kinetic Monte-Carlo (KMC) algorithm for spin flip Arrhenius dynamics, see Sect.4. In this section we present numerical experiments using potentials similar to those discussed in Sect.3.2 and Sect.3.3 to emphasize the importance of multi-body interactions. Also numerical results show the effectiveness of the potential splitting method, discussed in Sect.3.6.

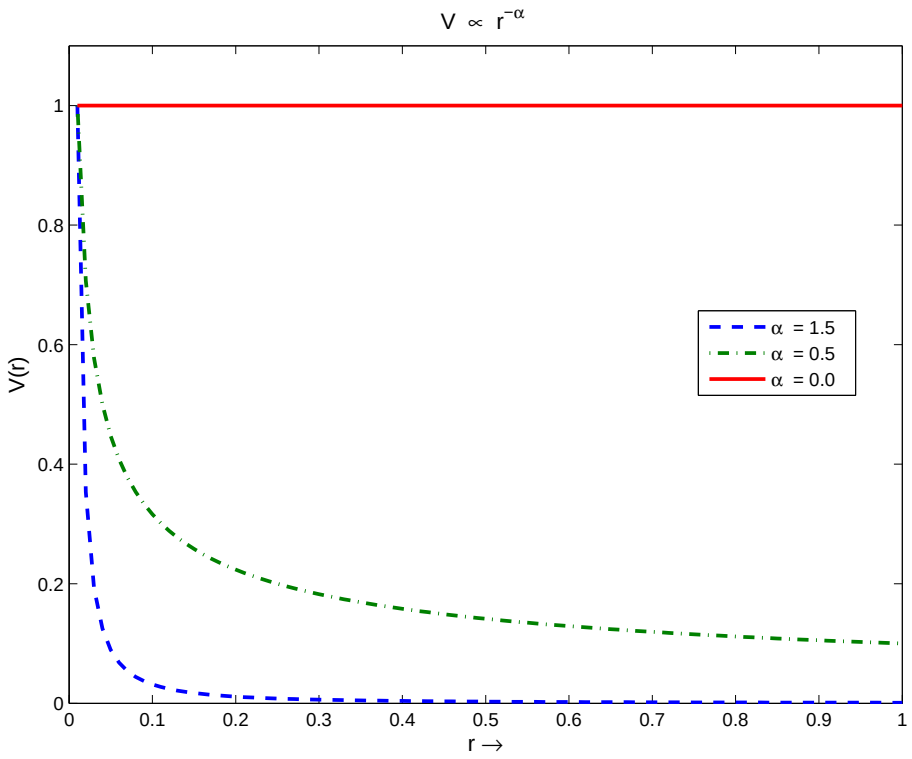


FIG. 5.1. *Different decaying potentials* $\propto r^{-\alpha}$ *with different values of* $\alpha$

**5.1. Power law potentials.** Fig.5.1 depicts examples of different long range potentials with an algebraic decay more specifically, they are of the following type,

$$J(x-y) = \frac{1}{N} V\left(|x-y|\right), \; x, y \in \Lambda. \tag{5.1}$$

where,

$$V(r) = \frac{K}{|r|^{\alpha}}, \;\; \text{if } |r| > 0; \tag{5.2}$$

and the constant $K$ is such that the total mass is kept fixed:

$$\frac{J_0}{2} = \frac{1}{N}\sum_{i=1}^{N} V(\frac{i}{N}) = \sum_{i=1}^{N} \frac{KN^{\alpha-1}}{i^{\alpha}} = K\sum_{i=1}^{N} \frac{N^{\alpha-1}}{i^{\alpha}}$$

We compute isotherms similarly to natural parameter continuation, i.e., we trace the magnetization vs. external field h, first upon increasing the field h from low values and then decreasing it from high values. In particular we look at the two cases, $\alpha = 0.8$ and $\alpha = 1.5$, for which we study hysteresis. In the numerical tests presented here we demonstrate that the derived corrections improve this behavior even in the case of nearest-neighbor interactions or high coarse-graining ratio $q$. The sampling of the equilibrium measure is done by using microscopic and coarse-grained Arrhenius dynamics discussed in Sect.4. It is observed in the numerical experiments that the multi-body terms which are given by $j^2_{klm}$ are more important for higher values of $\alpha$. It is observed that in the case when $\alpha = 0.8$, see Fig.5.2, the 2nd-order coarse-graining Scheme 2.1 is very good approximation even for high levels of coarse-graining ($q$) whereas in the case $\alpha = 1.5$, see Fig.5.3, the 2nd-order coarse-graining Scheme 2.1 is not sufficient. For larger values of $q$ the 3rd-order Scheme 2.2 appears to be much better approximation than 2nd-order coarse-grainingScheme 2.1 as $q$ increases.

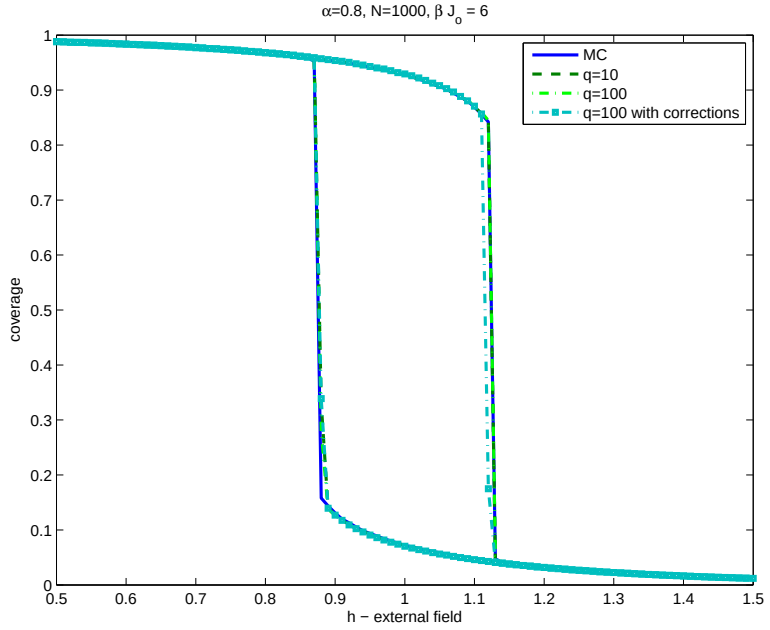


FIG. 5.2. *Comparison of different fully resolved(MC), coarse-grained $q = 10$, coarse-grained $q = 100$ and coarse-grained $q = 100$ with corrections. The potential here is the decaying potential as in* (5.1) *with $\alpha = 0.8$. Clearly, corrections due to three-body terms have minimal impact as Scheme 2.1 is already performing well.*

**5.2. Lennard-Jones type potential and potential splitting.** Another potential we consider is a Lennard-Jones type potential in which the short range interactions are repulsive and the long range interactions are attractive interactions. This type of potentials which involve combination of short and long range interactions

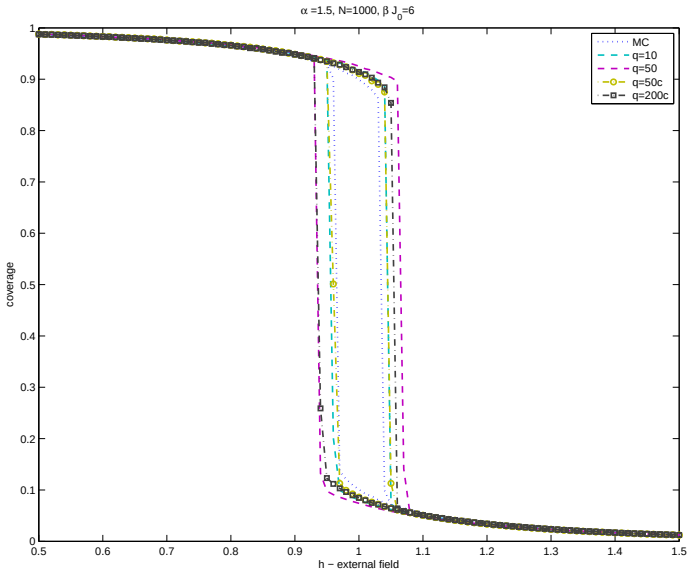


FIG. 5.3. *Comparison of different simulations fully resolved (MC), coarse-grained* $q = 10$*, coarse-grained* $q = 50$*, coarse-grained* $q = 50$ *with corrections,coarse-grained* $q = 200$ *with corrections. The potential here is the decaying potential as in* (5.1) *with* $\alpha = 1.5$.

are realistic in many lattice and off-lattice systems in fields like epitaxial growth or macromolecular systems. The potential used in the tests is given by

$$J(x-y) = \begin{cases} \dfrac{1}{3}\left(\dfrac{\sigma}{|x-y|} - \dfrac{\sigma^2}{|x-y|^2}\right), & |x-y| \le \sigma \\ \dfrac{K}{N}\left(\dfrac{\sigma}{|x-y|} - \dfrac{\sigma^2}{|x-y|^2}\right), & |x-y| > \sigma \end{cases} \qquad x, y \in \Lambda \tag{5.3}$$

where $K$ is such that $\frac{J_o}{2} = \sum_{i=1}^{N/2} J(i)$ and $\sigma = \frac{3}{N}$ . We insert here an $\frac{1}{N}$ dependence on the long range piece so that we can keep the total strength of the interaction fixed as $N \to \infty$.

The microscopic system ($q = 1$) exhibits at low temperature, Fig.5.5, a complex hysteresis diagram exhibiting a double hysteresis separated by an anti-ferromagnetic region; in these microscopic simulations we have also tested for finite size effects by testing various lattice sizes. Coarse-graining Scheme 2.1 fails to capture this behavior, while Scheme 2.2 does a much better job resolving the anti-ferromagnetic region; furthermore it predicts the double hysteresis but in shifted location. In Fig.5.5 we present the hysteresis using the potential given by (5.3) for the microscopic process, coarse-grained process with $q = 8$ and coarse-grained process with $q = 8$ and corrections. One of the problems implementing the 3rd-order scheme is that it is computationally expensive because of the number of multi-body terms, for example the $j^2_{klm}$ is a matrix of size $128 \times 128$. To overcome this problem as we discussed in Sect.3.6 we break up the potential into a short range piece and a smooth long range piece with $r_c = 16$, we do this realizing that because of the smoothness of the long range piece the error from coarse-graining is small, see Sect.3.3 . In Fig.5.4 we present the hysteresis diagram using the potential splitting and applying Scheme 2.2 just for the short range piece and Scheme 2.1 for the long range piece. It is observed that the predictions using the

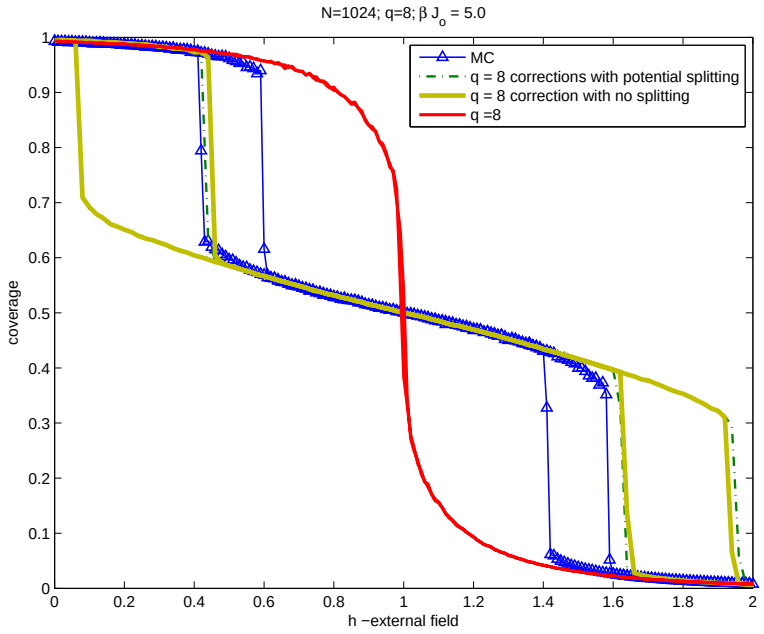


FIG. 5.4. *Comparison of hysteresis using a Lennard-Jones type potential of the microscopic process (MC), coarse-grained process $q = 8$, the coarse-grained process $q = 8$ with corrections using the full potential and the coarse-grained process $q = 8$ with corrections using the split potential for $\beta J_0 = 5.0$.*

potential splitting the hysteresis results are very similar to the results from no splitting of the potential. This shows that splitting the potential appropriately presents us an efficient way of including the multi-body terms and reduce the computational complexity of the multi-body terms. In Fig.5.5 we present the hysteresis results with the same setup as in Fig.5.4 expect at higher temperatures. We observe that the accuracy of the Scheme 2.1 as well as Scheme 2.2 is better a higher temperature. This is expected because the multi-body interactions are proportional to $\beta^2$ which results in smaller corrections at higher temperatures.

**5.3. Pathwise agreement and auto correlations.** In Fig.5.6 and Fig.5.7 we show the impact of the corrections on the dynamics of the coarse-grained process. The potential used here is a piecewise constant potential with an interaction radius $L = 100$, as discussed in Sect.3.1. The temperature is $\beta J_0 = 4.35$, we choose this temp close to the critical temperature so that we have enough noise in the system to generate short jumps.

In Fig.5.6 we compare the time series of the coarse-graining with and without corrections to the time series of the microscopic process (path wise agreement). The time series for each process is generated for a fixed time and sampling interval of $dt$ using the same sequence of random numbers. The comparison here is simply visual; a more statistically sound comparison would comparing the autocorrelation of the time series. In Fig.5.7 we compare the auto correlations of the time series of the coarse-graining with and without corrections to the auto correlation of the time series of the microscopic process. These simulations also study how well the different coarse-graining schemes approximate the microscopic process, especially the noise. The auto

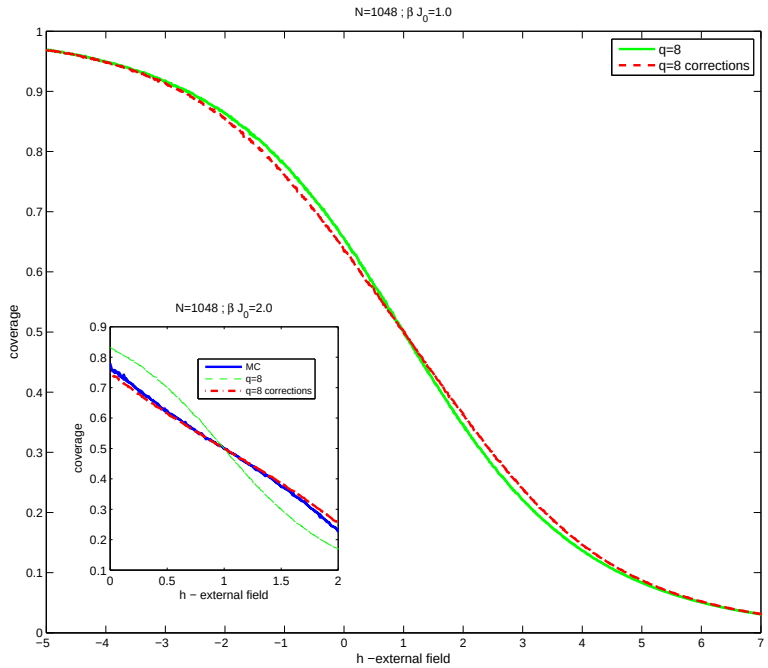


FIG. 5.5. *Comparison of hysteresis using a Lennard-Jones type potential of the microscopic process (MC), coarse-grained process $q = 8$ and the coarse-grained process $q = 8$ with corrections for $\beta J_0 = 1.0$. The inset is the comparison for $\beta J_0 = 2.0$. We note that Scheme 2.2 is appropriate at lower temperatures.*

correlation of time series $\{X_t\}$ as function of lag $h$ is defined as,

$$\gamma(h) = \frac{\mathbb{E}[(X_{t+h} - \nu)(X_t - \nu)]}{\mathbb{E}[(X_t - \nu)^2]}$$

where $\nu = \mathbb{E}[X_t]$. Note that $t$ here is equilibrated.

These simulations show that when coarse-graining microscopic systems with long range interactions the multi-body terms in the higher order coarse graining schemes are important to capture the correct dynamical behavior of the microscopic process. This is in fact true even in regimes where equilibrium properties like hysteresis were predicted accurately without including the multi-body terms (see Fig.3 in[14]). Also these simulations show that we are able to accurately compress the long range interactions on the microscopic lattice to nearest neighbor interactions on the coarse lattice and hence improving the computational cost of the coarse-graining.

**5.4. Mean time to reach phase transition.** We use the coarse-graining schemes described and analyzed in the previous sections for efficient simulations in the spin systems that undergo phase transitions. Within the context of spin-flip dynamics a typical example is nucleation of spatial regions of a new phase or a transition from one phase (all spins equal to zero) to another (all spins equal to one). In such simulations the emphasis is on the pathwise properties of the coarse-grained process so that the switching mechanism is simulated efficiently while approximation errors are controlled. We compare simulations on the microscopic level with those performed on different levels of coarse-graining hierarchy parametrized by $q$. A quantity of interest

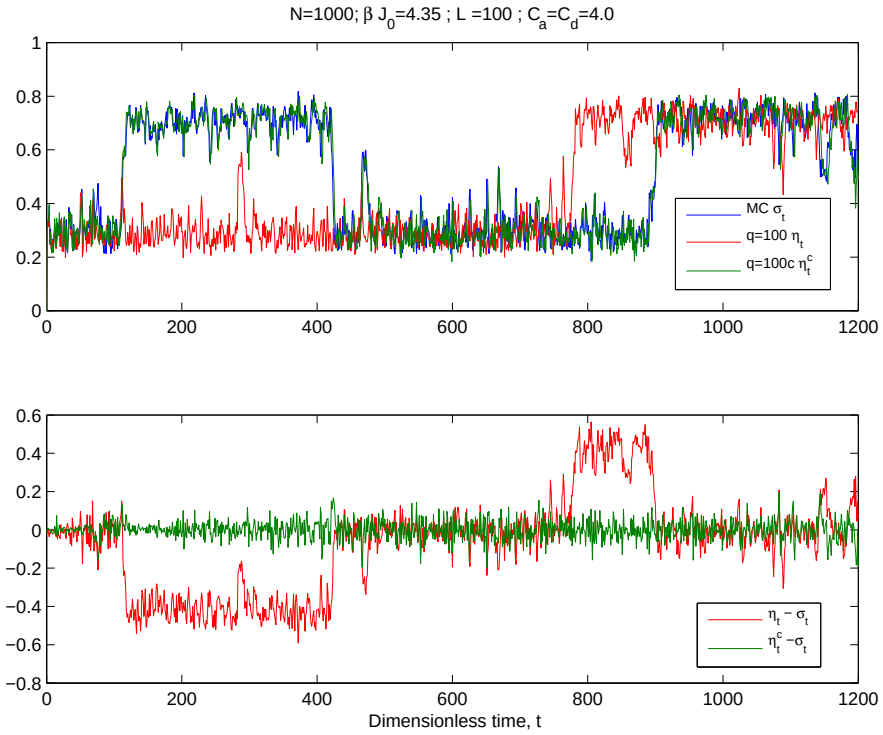


FIG. 5.6. *Comparison of the time series for the cases of fully resolved microscopic process (MC), coarse-grained ($q = 100$) and coarse-grained with corrections ($q = 100c$). The potential is a piecewise constant potential with interaction range is $L = 100$ and $\beta J_0 = 4.35$.*

that is calculated is the meantime $\bar{\tau}_T = E[\tau_T]$ which is defined as the time until the coverage reaches $C^+$ in its phase transition regime. The random exit time is defined as $\tau_T = \inf\{t > 0 \,|\, c_t \geq C^+\}$. We estimate the microscopic probability distributions $\rho_\tau$ and $\rho_\tau^q$ from the simulations. We record a phase transition at the time $\tau_T$ when the coverage exceeds the threshold value $C^+ = 0.9$. The potential used in these simulations is a piecewise potential with an interaction radius $L = 100$ and $\beta J_0 = 6.0$. Note that $\beta J_0 = 6$, which is above the critical value of 4.0, is a bistable regime where two phases can coexist. Changing the external field $h$ creates fluctuations that allow for transitions between the equilibrium. In these simulations the emphasis is on the pathwise properties of the coarse-grained process so that the switching mechanism from one stable state to another is simulated efficiently. In Table 5.1 we look at a relative error of the mean exit time $\bar{\tau}_T = E[\tau_T]$ for different levels of coarse-graining and we observe that the relative error from Scheme 2.1 increases with the size of the coarse-graining. In Table 5.1 we also present the results from the simulations using Scheme 2.2 and observe that even at high levels of coarse-graining in the 3rd-order scheme the relative error of the mean exit times is very small. In Fig.5.8 we plot approximations of the probability density functions (PDFs) of $\tau_T$ and compare them to the microscopic PDF for different values of coarse-graining $q$ and the respective corrections. It is demonstrated that including the multi-body interactions improves the PDF's substantially. In Table 5.2 and Fig.5.9 we present results from simulations that were carried under same condition but at a different (lower) temperature. The

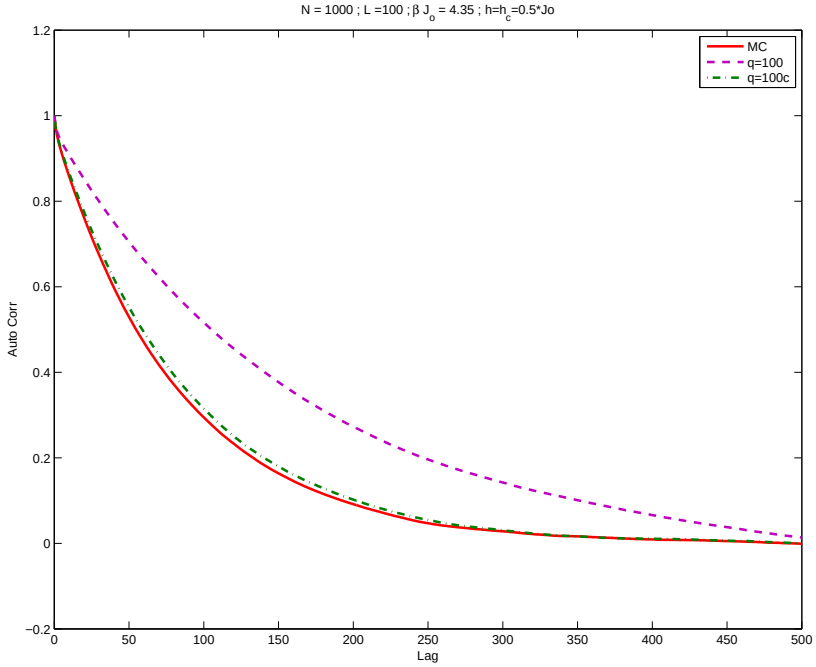


FIG. 5.7. *Auto correlation of the time series for the cases fully resolved $q = 1$(MC), coarse-grained $q = 100$ and coarse-grained with corrections $q = 100$. The potential is a piecewise constant potential with interaction range is $L = 100$ and $\beta J_0 = 4.35$.*

results for the higher order scheme qualitatively show an improvement. However, we observe a higher error in the case of lower temperature. This is expected because $\epsilon$, defined in (3.1), depends on the temperature $\beta$.

TABLE 5.1
*Approximation of $\bar{\tau}_T$ , $\|\rho_\tau^q - \rho_\tau\|_{L^1}$ and relative error. Measurements based on averaging over 10000 independent realizations for each $q$.*

$N = 1000$, $\beta J_0 = 6.0$, $h = 0.4406$

CGMC without corrections

| $L$ | $q$ | $\bar{\tau}_T$ | $\|\rho_\tau^q - \rho_\tau\|_{L^1}$ | Rel. Err. |
|---|---|---|---|---|
| 100 | 1 | 486.91 | 0 | 0 |
| 100 | 10 | 491.69 | 0.0022 | 1.16% |
| 100 | 20 | 503.96 | 0.0025 | 3.68% |
| 100 | 25 | 511.67 | 0.0032 | 5.27% |
| 100 | 50 | 584.08 | 0.0074 | 20.17% |
| 100 | 100 | 980.92 | 0.0246 | 101.82% |

CGMC with corrections

| $L$ | $q$ | $\bar{\tau}_T$ | $\|\rho_\tau^q - \rho_\tau\|_{L^1}$ | Rel. Err. |
|---|---|---|---|---|
| 100 | 50 | 480.78 | 0.0025 | 1.08% |
| 100 | 100 | 479.00 | 0.0028 | 1.45% |

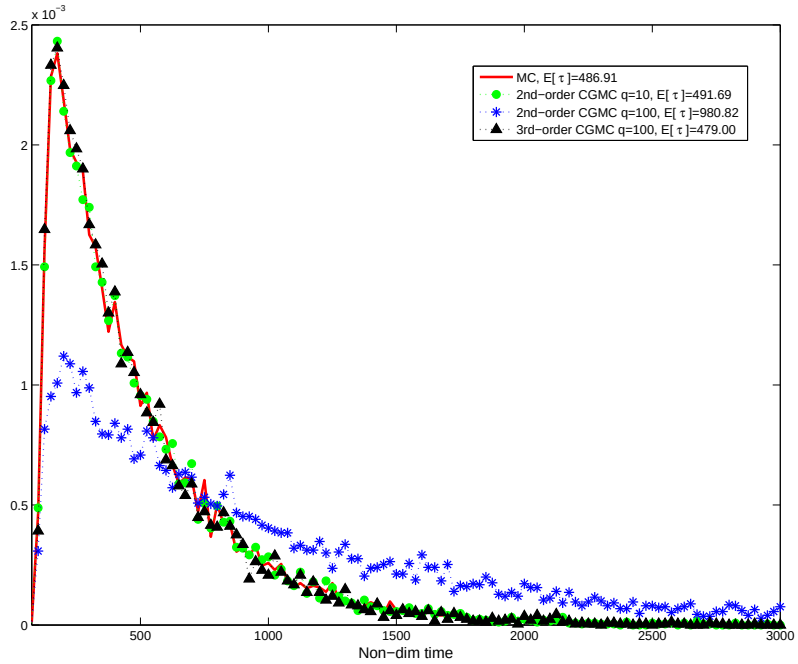


FIG. 5.8. *Probability density function(PDFs) comparisons between different coarse-graining levels $q$. The estimated meantimes for each PDF are shown in the figures. All PDFs comprised of 10000 samples and the histogram is approximated by 200 bins. The potential is a piecewise constant potential with interaction range is $L = 100$ and $\beta J_0 = 5.0$.*

TABLE 5.2

*Approximation of $\bar{\tau}_T$ , $\|\rho_\tau^q - \rho_\tau\|_{L^1}$ and relative error. Measurements based on averaging over 10000 independent realizations for each $q$.*

$N = 1000$, $\beta J_0 = 8.0$, $h = 0.38375$

CGMC without corrections

| $L$ | $q$ | $\bar{\tau}_T$ | $\|\rho_\tau^q - \rho_\tau\|_{L^1}$ | Rel. Err. |
|---|---|---|---|---|
| 100 | 1 | 367.89 | 0 | 0 |
| 100 | 10 | 379.39 | 0.0032 | 3.13% |
| 100 | 20 | 398.25 | 0.0038 | 8.25% |
| 100 | 25 | 416.05 | 0.0046 | 13.09% |
| 100 | 50 | 569.43 | 0.0131 | 54.78% |
| 100 | 100 | 1482.23 | 0.0416 | 302.9% |

CGMC with corrections

| $L$ | $q$ | $\bar{\tau}_T$ | $\|\rho_\tau^q - \rho_\tau\|_{L^1}$ | Rel. Err. |
|---|---|---|---|---|
| 100 | 50 | 335.94 | 0.0042 | 8.68% |
| 100 | 100 | 290.64 | 0.0072 | 21.00% |

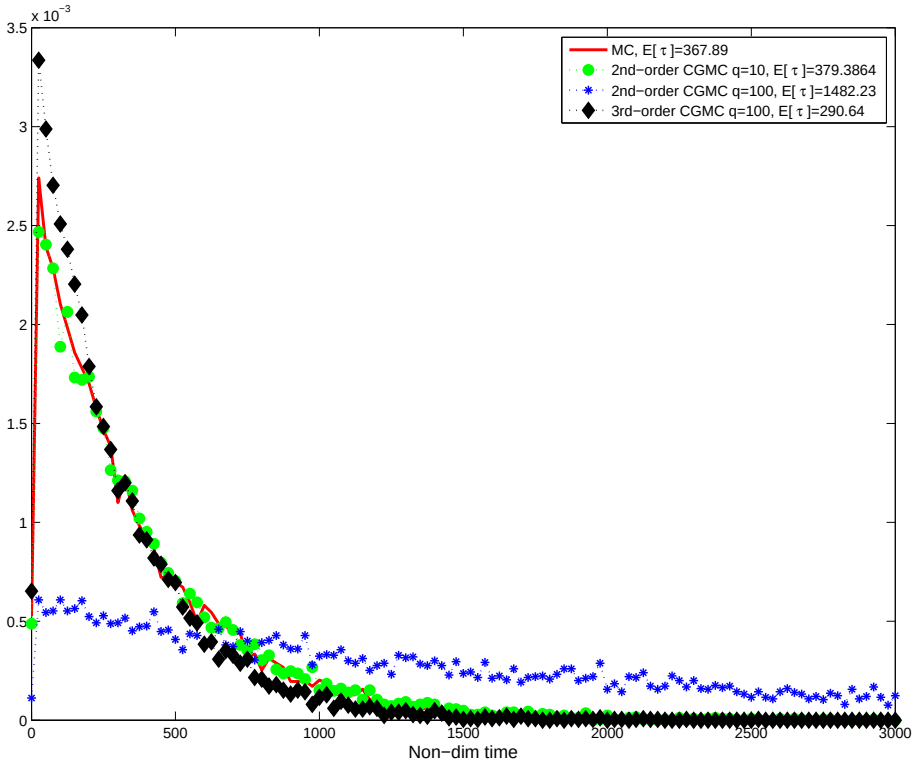


FIG. 5.9. *Probability density function(PDFs) comparisons between different coarse-graining levels q. The estimated meantimes for each PDF are shown in the figures. All PDFs comprised of 10000 samples and the histogram is approximated by 200 bins. The potential is a piecewise constant potential with interaction range is* $L = 100$ *and* $\beta J_0 = 8.0$.

**6. Connections to coarse-graining of polymer chains: The McCoy-Curro scheme.** So far we have studied coarse-graining of lattice based systems with a focus on understanding the error from coarse-graining and methodology that will enable deriving higher order schemes when required. Next we proceed to explore the connections and implications of these methodologies to coarse-graining of macromolecular systems. Coarse-graining of macromolecular systems has attracted considerable attention in polymer science and engineering [17, 19]; key challenges include the presence of complex short and long-range interactions, as well as the off-lattice nature of the models. In this section we discuss the connections and extensions the analytical and computational strategies for coarse-graining lattice systems presented in this paper as well as in [10, 14, 12] to more complex off-lattice macromolecular systems, specifically coarse-graining of polymer systems.

**6.1. McCoy-Curro scheme for off lattice systems.** We first present a coarse-graining procedure from the UA model which is known in the polymer science coarse-graining literature as the McCoy-Curro scheme [2, 5, 7, 22]. This scheme was first developed for the coarse-graining of small molecules in [18] and later extended to polymers by [5]. The interactions in the system consist of bonded interactions ($H_b$) which are *short-range* interactions between neighboring atoms in an individual polymer chain; they are defined via a potential $U_b$ which is a function of the bond length $r$, the bond angle $\Theta$ and the torsion angle $\Phi$, i.e. $H_b = \sum U_b(r, \Theta, \Phi)$. The interactions consist also of non-bonded ($H_{nb}$) which are *long-range* interactions between atoms of different chains and are typically modelled with a Lennard-Jones(LJ) two body potential $U_{nb}$. The Hamiltonian also includes total kinetic energy ($H_{kin}$) of the system, Coulomb interactions ($H_{coul}$)associated with charged macromolecules and terms which describe the interactions associated with walls ($H_{wall}$). The total UA model consists of $n$ macromolecules in a fixed volume at the inverse temperature $\beta$ and each macro molecule consists of $m$ atoms. Hence the system consists of $N = nm$ microscopic particles denoted by $X = (x_1, \ldots, x_N)$, where $x_i \in \mathbb{R}^3$ is the position of the $i$th atom. The Hamiltonian of the system is given by,

$$H_N(X) = H_b(X) + H_{nb}(X) + H_{coul}(X) + H_{wall}(X) + H_{kin}(X) \tag{6.1}$$

The corresponding canonical Gibbs measure is given by,

$$\mu(dX) = \frac{1}{Z} e^{-\beta H_N(X)} \prod_i dx_i \,, \quad Z = \int_X e^{-\beta H_N(X)} \prod_i dx_i \tag{6.2}$$

The coarse-graining of this system is carried out by grouping $q$ of the united atoms together by creating a chain consisting of $M = N/q$ "super-atoms". The CG particles are denoted by the coarse variables $Q = (q_1, \ldots, q_M)$, where $q_i \in \mathbb{R}^3$ is the position of the centre of mass $i^{th}$ super-atom. Just as in the lattice case the focus here is to derive the coarse-grained Hamiltonian and the corresponding coarse-grained interaction potentials. The exact coarse-grained Hamiltonian $\bar{H}_M(Q)$ is defined as in the lattice case (see (2.7)) ,

$$e^{-\beta \bar{H}_M(Q)} = \int_{\{X \in \mathbf{X} | \mathbf{F}X = Q\}} e^{-\beta H_N(X)} \, dX. \tag{6.3}$$

where $\mathbf{F}$ denotes the projection of the microscopic variable to the coarse variable.

For the sake of simplicity we focus on the case where only bonded and non-bonded interactions are present in the Hamiltonian, i.e., $H_N(X) = H_b(X) + H_{nb}(X)$. From

(6.3) we have,

$$\bar{H}_M(Q) = -\frac{1}{\beta}\log\int_{\{X\in\mathbf{X}|\mathbf{F}X=Q\}} e^{-\beta(H_b(X)+H_{nb}(X))}\,dX. \tag{6.4}$$

Although (6.4) is not additive, we assume that $\bar{H}_M = \bar{H}_b(X) + \bar{H}_{nb}$, where $\bar{H}_b(X)$, $\bar{H}_{nb}$ are the coarse-grained versions of the bonded and non-bonded interactions, $H_b$ and $H_{nb}$. Furthermore, we assume $\bar{H}_b = \sum \bar{U}_b$ and $\bar{H}_{nb} = \sum \bar{U}_{nb}$ respectively where $\bar{U}_b$ and $\bar{U}_{nb}$ are the corresponding CG potentials. It is assumed that $\bar{U}_b(r,\Theta,\Phi)$ can be furthered simplified and can be written as, $\bar{U}_b(r,\Theta,\Phi) = \bar{U}_b^r + \bar{U}_b^\Theta + \bar{U}_b^\Phi$. Similarly, it is assumed the long-range term $\bar{U}_{nb}$ depends only on binary interactions between coarse-graine particles and is given by the average of the interactions between two isolated molecules at positions $q_i, q_j$,

$$\bar{U}_{nb}(|q_i - q_j|) = -\frac{1}{\beta}\log\int_{\{X:\mathbf{F}X=(q_i,q_j)\}} e^{-\beta\tilde{H}_{nb}}dX. \tag{6.5}$$

where the Hamiltonian $\tilde{H}_{nb}$ is the detailed description of two isolated molecules. In other words, $\bar{U}_{nb}(|q_i - q_j|)$ is just two-body coarse-graine interaction.

**6.2. McCoy-Curro scheme on the lattice.** To further understand the McCoy-Curro scheme, we present the scheme in the context of lattice systems drawing some analogies between the coarse-graining of polymer chains and coarse-graining in lattice systems. An important fact that is highlighted in Sect.3 is the role of the multi-body interactions when studying complex interactions which are absent in the present coarse-graining methods applied to macromolecular systems (see (6.5)). According to the McCoy-Curro scheme the coarse-grained Hamiltonian is given by,

$$\bar{H}^{MCC}(\eta) = -\sum_{k,\,l\in\bar{\Lambda}_M} \bar{U}^{MCC}(\eta_k,\eta_l,|k-l|) \tag{6.6}$$

where in analogy to (6.5):

$$\bar{U}^{MCC}(\eta_k,\eta_l,|k-l|) = -\frac{1}{\beta}\ln(\mathbb{E}\left[e^{-\beta H_{C_k,C_l}(\sigma)}|\eta_k,\,\eta_l\right]) \tag{6.7}$$

where

$$H_{C_k,C_l}(\sigma) = -\frac{1}{2}\sum_{x\in C_k,\,y\in C_l} J(x-y)\sigma(x)\sigma(y) \tag{6.8}$$

The definition of $H_{C_k,C_l}(\sigma)$ given by (6.8) assumes that the interaction between two molecules (coarse cells) is independent of configuration of other molecules in the polymer. If we rewrite the $U^{MCC}(\eta_k,\eta_l,|k-l|)$ defined in (6.7) in terms $\bar{J}(k,l)$, we get

$$\begin{aligned}\bar{U}^{MCC}(\eta_k,\eta_l,|k-l|) &= \frac{1}{2}\bar{J}(k,l)\,\eta_k\,\eta_l - \frac{1}{\beta}\ln(\mathbb{E}[e^{(-\beta\Delta J_{kl}(\sigma))}|\eta_k,\,\eta_l]) \\ &= \frac{1}{2}\bar{J}(k,l)\,\eta_k\,\eta_l - \frac{1}{\beta}\ln(\int_{\{\sigma:\mathbf{F}(\sigma)=(\eta_k,\eta_l)\}} e^{(-\beta\Delta J_{kl}(\sigma))}P(d\sigma|\eta_k,\,\eta_l))\end{aligned} \tag{6.9}$$

The equation (6.9) is similar to (2.9) however it is not defined on the entire lattice. Using a Taylor expansion, note that this system is not extensive hence there is no

need for cluster expansions, of the second term on the right hand side of (6.9) we have that,

$$\begin{aligned}
\bar{H}^{MCC}(\eta) &= -\sum_{k,\, l\in\bar{\Lambda}_M}\left\{\frac{1}{2}\bar{J}(k,l)\,\eta_k\,\eta_l - \frac{1}{\beta}\ln\Big(\int_{\{\sigma:\mathbf{F}(\sigma)=(\eta_k,\eta_l)\}} e^{(-\beta\Delta J_{kl}(\sigma))}P(d\sigma|\eta_k,\,\eta_l)\Big)\right\}\\
&= -\sum_{k,\, l\in\bar{\Lambda}_M}\frac{1}{2}\bar{J}(k,l)\,\eta_k\,\eta_l + \sum_{k,l}\frac{1}{\beta}\ln(\mathbb{E}[e^{(-\beta\Delta J_{kl}(\sigma))}\ \ |\eta_k,\,\eta_l)])\\
&= -\sum_{k,\, l\in\bar{\Lambda}_M}\frac{1}{2}\bar{J}(k,l)\,\eta_k\,\eta_l + \sum_{k,l}\frac{1}{\beta}\ln[1+\mathbb{E}[(-\beta\Delta J_{kl}(\sigma))^2]+\dots]\\
&= -\sum_{k,\, l\in\bar{\Lambda}_M}\frac{1}{2}\bar{J}(k,l)\,\eta_k\,\eta_l + \sum_{k,l}\frac{\beta}{2}\mathbb{E}[(\Delta J_{kl}(\sigma))^2]+\dots\\
&= \bar{H}^{(0)}_M(\eta)+\bar{H}^{(1)}_M(\eta)+\dots(\text{ higher-order two-body interactions}) \qquad (6.10)
\end{aligned}$$

It is clear that from the above calculations that the McCoy-Curro scheme is asymptotically identical to the using $\bar{H}^0_M(\eta)$ and $\bar{H}^1_M(\eta)$ given in Sect.2.4. However the three body terms given by $\bar{H}^2_M(\eta)$ are obviously absent. As we have seen in Sect.3 and Sect.5, including 3-body interactions is crucial to obtain higher accuracy, especially in low temperature regimes. At the same time in Sect.3 and Sect.5 we have shown how to effectively incorporate such possibly costly terms in the coarse-graining algorithm.

Remark 3. It should also be noted that from a computational point of view the schemes in Sect.2.4 are much more efficient than the McCoy-Curro scheme, as implementing the McCoy-Curro scheme requires calculating $\bar{U}^{CG}(\eta_k,\eta_l,|k-l|)$ using (6.7) over all possible ranges of $\eta_k,\eta_l,|k-l|$ and repeating all the calculations for each temperature $\beta$. It is not our contention that the higher order terms which involve interactions between more than two molecules of polymer cannot be done using the McCoy-Curro scheme but the increase in computational cost will be significant and without a clear understanding when they are important, unless a similar analysis to Sect.3 is performed.

REFERENCES


[1] C. F. Abrams and K. Kremer, *The effect of bond length on the structure of dense bead–spring polymer melts*, The Journal of Chemical Physics, 115 (2001), pp. 2776–2785.

[2] R. L. C. Akkermans and W. J. Briels, *Coarse-grained interactions in polymer melts: A variational approach*, The Journal of Chemical Physics, 115 (2001), pp. 6210–6219.

[3] A. Chatterjee and D. Vlachos, *An overview of spatial microscopic and accelerated kinetic monte carlo methods*, Journal of Computer-Aided Materials Design, 14 (2007), pp. 253–308.

[4] T. M. Cover and J. A. Thomas, *Elements of information theory*, Wiley Series in Telecommunications, John Wiley & Sons Inc., New York, 1991. , A Wiley-Interscience Publication.

[5] H. Fukunaga, J. ichi Takimoto, and M. Doi, *A coarse-graining procedure for flexible polymer chains with bonded and nonbonded interactions*, The Journal of Chemical Physics, 116 (2002), pp. 8183–8190.

[6] N. Goldenfeld, *Lectures on Phase Transitions and the Renormalization Group*, vol. 85, Addison-Wesley, New York, 1992.

[7] V. A. Harmandaris, N. P. Adhikari, N. F. A. van der Vegt, and K. Kremer, *Hierarchical modeling of polysterene: From atomistic to coarse-grained simulations*, Macromolecules, 39 (2006), p. 6708.

[8] L. Kadanoff, *Scaling laws for ising models near $t_c$*, Physics, 2 (1966), p. 263.

[9] M. Kardar, *Crossover to equivalent-neighbor multicritical behavior in arbitrary dimensions.*, Phys. Rev. B, 28 (1983), pp. 244–246.

[10] M. A. Katsoulakis, A. J. Majda, and D. G. Vlachos, *Coarse-grained stochastic processes and Monte Carlo simulations in lattice systems.*, J. Comp. Phys., 112 (2003), pp. 250–278.

[11] M. A. Katsoulakis, A. J. Majda, and D. G. Vlachos, *Coarse-grained stochastic processes for microscopic lattice systems*, Proc. Natl. Acad. Sci. USA, 100 (2003), pp. 782–787 (electronic).

[12] M. A. Katsoulakis, P. Plechac, L. Rey-Bellet, and D. K. Tsagkarogiannis, *Mathematical strategies in the coarse-graining of extensive systems: Error quantification and adaptivity;*, Journal of Non-Newtonian Fluid Mechanics, In Press,.

[13] M. A. Katsoulakis, P. Plecháč, and A. Sopasakis, *Error analysis of coarse-graining for stochastic lattice dynamics*, SIAM J. Numer. Anal., 44 (2006), pp. 2270–2296 (electronic).

[14] M. A. Katsoulakis, L. Rey-Bellet, P. Plecháč, and D. Tsagkarogiannis, *Coarse-graining schemes and a posteriori error estimates for stochastic lattice systems*, Mathematical Modelling and Numerical Analysis, 41 (2006), pp. 327–660.

[15] M. A. Katsoulakis and A. Szepessy, *Stochastic hydrodynamical limits of particle systems*, Commun. Math. Sci., 4 (2006), pp. 513–549.

[16] M. A. Katsoulakis and J. Trashorras, *Information loss in coarse-graining of stochastic particle dynamics*, J. Stat. Phys., 122 (2006), pp. 115–135.

[17] K. Kremer and F. Müller-Plathe, *Multiscale problems in polymer science: simulation approaches*, MRS Bull., (March 2001), p. 205.

[18] J. McCoy and J. Curro, *Mapping of explicit atom onto united atom potentials*, Macromolecules, 31 (1998), pp. 9362–9368.

[19] F. Müller-Plathe, *Coarse-graining in polymer simulation: from the atomistic to the mesoscale and back*, Chem. Phys. Chem., 3 (2002), p. 754.

[20] I. Pivkin and G. Karniadakis, *Coarse-graining limits in open and wall-bounded dissipative particle dynamics systems*, J. Chem. Phys., 124 (2006), p. 184101.

[21] B. Simon, *The statistical mechanics of lattice gases. Vol. I*, Princeton Series in Physics, Princeton University Press, Princeton, NJ, 1993.

[22] W. Tschöp, K. Kremer, O. Hahn, J. Batoulis, and T. Bürger, *Simulation of polymer melts. I. coarse-graining procedure for polycarbonates*, Acta Polym., 49 (1998), p. 61.

[23] B. Turkington, *Statistical equilibrium measures and coherent states in two-dimensional turbulence*, Comm. Pure Appl. Math., 52 (1999), pp. 781–809.

## APPENDIX A.

**AI. Piecewise constant potential.** Before we proceed to study general potentials, we analyze piecewise constant potential which is widely used in simulations as a benchmarks. Note that even though we present this discussion of the piecewise constant in one dimension, it can be easily extended to higher dimensions. Suppose that $V(r) = \frac{J_0}{2}$ for $|r| \leq 1$ and $J$ is given by (2.1), (**??**) with interaction radius $L$, i.e. $J(x-y) = \frac{J_0}{2L}$ when $|x-y| \leq L$. Assume that the coarse-graining level is $q$ and the coarse length of the interaction $\bar{L} = \dfrac{L}{q} \in \mathbb{Z}$, then it follows by simple counting,

1. For $x \in C_k$ and $y \in C_l$,

$$\text{if } |k-l| < \frac{L}{q} - 1, \qquad |J(x,y) - \bar{J}(k,l)| = 0 \tag{A.I}$$

$$\text{if } |k-l| = \frac{L}{q} - 1, \qquad |J(x,y) - \bar{J}(k,l)| = \begin{cases} \dfrac{J_0}{2L}\dfrac{(q-1)}{2q} & \text{when } |x-y| \leq L \\ \dfrac{J_0}{2L}\dfrac{(q+1)}{2q} & \text{when } |x-y| > L \end{cases} \tag{A.II}$$

$$\text{if } |k-l| = \frac{L}{q}, \qquad |J(x,y) - \bar{J}(k,l)| = \begin{cases} \dfrac{J_0}{2L}\dfrac{(q^2-1)}{q^2} & \textit{when } |x-y| \leq L \\ \dfrac{J_0}{2L}\dfrac{1}{q^2} & \textit{when } |x-y| > L \end{cases} \tag{A.III}$$

2. If $\mathbf{F}(\sigma) = \eta$, we have

$$\frac{1}{N}\left|H_N(\sigma) - \bar{H}_M^{(0)}(\eta)\right| \leq \frac{M}{N}\left(\frac{J_0}{4L}(q^2-1) + \frac{J_0}{L}\left(\frac{2q-1}{q} + \frac{q-2}{q^2}\right)\right).$$

**AII. Decaying potential.** Assume that $J$ is given by (2.1) and $V(r) \in C^1(\Omega)$ satisfies

$$\begin{aligned} |V(r)| &\leq \frac{K}{r^\alpha} \\ |V'(r)| &\leq \frac{K\alpha}{r^{\alpha+1}} \end{aligned}, \quad \text{for } r > r_c; \tag{A.IV}$$

Then we have,

1. For all $k, l$ such that $r_{|k-l|} > r_c$,

$$|\bar{J}(k,l)| \leq \frac{K}{N}\frac{1}{(r_{|k-l|})^\alpha} \tag{A.V}$$

2. For all $k, l$ such that $r_{|k-l|} > r_c$ , if $x \in C_k$ and $y \in C_l$

$$|J(x,y) - \bar{J}(k,l)| \leq \frac{2K\alpha\sqrt{d}}{q^d m^{d+1}} \frac{1}{(r_{|k-l|})^{\alpha+1}} \tag{A.VI}$$

PROOF: By definition of $\bar{J}(k,l)$ we have that,

$$\begin{aligned} |\bar{J}(k,l)| &= \left| m^{2d} \iint_{x\in C_k \; y\in C_l} J(x,y)dxdy \right| \\ &\leq \sup_{x\in C_k \; y\in C_l} |J(x,y)| \\ &\leq \frac{K}{N} \frac{1}{(r_{|k-l|})^{\alpha}} \end{aligned}$$

Using the definition of $J$ in (2.1), $x \in C_k$ and $y \in C_l$, we have,

$$\begin{aligned} J(x,y) = \frac{1}{q^{2d}} \sum_{x'\in C_k} \sum_{y'\in C_l} J(x'-y') + \\ + \frac{1}{q^{2d}} \sum_{x'\in C_k} \sum_{y'\in C_l} \frac{1}{N}((x-y)-(x'-y')) \, .\nabla V(|\xi'_x - \xi'_y|) \end{aligned}$$

for some $\xi'_x \in C_k \;\; \xi'_y \in C_l$ .

$$\begin{aligned} \Rightarrow |J(x,y) - \bar{J}(k,l)| &\leq \frac{2\sqrt{d}}{q^d m^{d+1}} \sup_{x'\in C_k \; y'\in C_l} |\nabla V(|x'-y'|)| \\ &\leq \frac{2\alpha\sqrt{d}K}{Nm} \frac{1}{(r_{|k-l|})^{\alpha+1}} \, . \end{aligned}$$

Under the assumptions of example in Section3.2 and from the estimates (3.3) and (3.4), if $\mathbf{F}(\sigma) = \eta$, we have

$$\begin{aligned} \frac{1}{N} \left| H_N(\sigma) - \bar{H}_M^{(0)}(\eta) \right| \leq \; & \frac{1}{Q} \left( \sum_{\{l \, : \, r_l \leq r_c\}} \mathrm{D}_{r_l} \right) \\ & + \; \frac{4\pi^{\frac{d}{2}} K\alpha\sqrt{d}}{\Gamma(\frac{d}{2})m} \left[ \frac{1-(r_c)^{(d-1-\alpha)}}{(d-1-\alpha)} \right] . \end{aligned} \tag{A.VII}$$

PROOF: Using the above example in Section3.2 and the estimates from in (3.3) and (3.4) for $I_1$ we have,

$$\begin{aligned} I_1 &= \frac{1}{N} \sum_k \sum_{\{l \, : \, r_{|k-l|} \leq r_c\}} \left( \sum_{\substack{x\in C_k \\ y\in C_l, y\neq x}} |\mathrm{E}_{kl}(x,y)| \right) \\ &\leq \frac{1}{N} \sum_k \sum_{\{l \, : \, r_{|k-l|} \leq r_c\}} \mathrm{D}_{kl} \\ &\leq \frac{1}{Q} \left( \sum_{\{l \, : \, r_l \leq r_c\}} \mathrm{D}_{r_l} \right) \end{aligned}$$

Using (3.4) for $I_2$ we have,

$$\begin{aligned} I_2 &= \frac{1}{N}\sum_k \sum_{\{l\,:\,r_{|k-l|}>r_c\}} \left( \sum_{\substack{x\in C_k \\ y\in C_l, y\neq x}} |J(x,y)-\bar{J}(k,l)| \right) \\ &\leq \frac{1}{N}\frac{N}{q^d} q^{2d} \sum_{\{l\,:\,r_{0,l}>r_c\}} \frac{2K\alpha\sqrt{d}}{N^d m} \frac{1}{(r_{0,l})^{\alpha+1}} \\ &= \frac{2K\alpha\sqrt{d}}{m} \left( \frac{1}{m^d} \sum_{\{l\,:\,r_{0,l}>r_c\}} \frac{1}{(r_{0,l})^{\alpha+1}} \right) \\ &\leq \frac{2K\alpha\sqrt{d}}{m} \frac{2\pi^{\frac{d}{2}}}{\Gamma(\frac{d}{2})} \int_{r_c}^1 \frac{1}{r^{\alpha+1}} r^{d-1} dr \\ &= \frac{2K\alpha\sqrt{d}}{m} \frac{2\pi^{\frac{d}{2}}}{\Gamma(\frac{d}{2})} \left[ \frac{1-(r_c)^{(d-1-\alpha)}}{(d-1-\alpha)} \right]. \end{aligned}$$

Based on the above corollary the parameter $\epsilon$ is given by,

$$\begin{aligned} \epsilon &\equiv \beta \frac{1}{q^d} \left( \sum_{\{l\,:\,r_l\leq r_c\}} \mathrm{D}_{r_l} \right) + \beta \frac{2K\alpha\sqrt{d}}{m} \frac{2\pi^{\frac{d}{2}}}{\Gamma(\frac{d}{2})} \left[ \frac{1-(r_c)^{(d-1-\alpha)}}{(d-1-\alpha)} \right] \\ &:= \epsilon_s + \epsilon_l \,. \end{aligned}$$

where $\epsilon_s$ and $\epsilon_l$ represent the error made by coarse-graining the short range interactions and long range interactions respectively.

**AIII. Potentials with integrable singularity.** Another special kind of potentials are those with integrable singularity in higher dimensions (i.e. $r^{d-1}V'(r) \in L^1(\Omega)$) which describe potentials like Coulomb interactions where the interactions are inversely proportional to the distance in $\mathbb{R}^3$ [21] and turbulence in $\mathbb{R}^2$ where the interactions are proportional to the logarithm of the distance between two interacting sites[23].

Assume that $J$ is given by (2.1),(**??**), $V(r) \in C^1(\Omega)$ and $r^{d-1}V'(r) \in L^1(\Omega)$,

1. If $x \in C_k$ and $y \in C_l$, we have

$$|J(x,y)-\bar{J}(k,l)| \leq \frac{1}{N} \|r^{d-1}V'\|_{L^1(r_{kl}-\frac{\sqrt{d}}{m}, r_{kl}+\frac{\sqrt{d}}{m})} \tag{A.VIII}$$

2. If $\mathbf{F}(\sigma) = \eta$, we have

$$\frac{1}{N}\left| H_N(\sigma) - \bar{H}_M^{(0)}(\eta) \right| \leq \left( \frac{1}{M} \|r^{d-1}V'\|_{L^1} \right) \tag{A.IX}$$

PROOF: By definition of $\bar{J}(k,l)$ we get,

$$\begin{aligned}
|J(x,y) - \bar{J}(k,l)| &= \left| M^2 \int_{C_k}\int_{C_l} (J(x-y) - J(r-s)) dr\, ds \right| \\
&\le M^2 \int_{C_k}\int_{C_l} |J(x-y) - J(r-s)|\, dr\, ds \\
&\le M^2 \int_{C_k}\int_{C_l} \left| \int_0^1 \nabla J(\gamma(t)) \cdot \gamma'(t) dt \right| dr\, ds \\
&\qquad \text{where } \gamma(t) = (1-t)(r-s) + t(x-y)\,. \\
&\le \frac{2\sqrt{d}\, M^2}{m} \int_0^1 \int_{C_k}\int_{C_l} \frac{1}{N} |V'(|\gamma(t)|)|\, ds\, dr\, dt \\
&\le \frac{4\sqrt{d}\,\pi^{d/2}\, M^2}{m\, N} \int_0^1 \int_{C_k} \int_{r_{kl}-\frac{\sqrt{d}}{m}}^{r_{kl}+\frac{\sqrt{d}}{m}} z^{d-1} |V'(z)|\, dz\, dr\, dt \\
&\le \frac{4\sqrt{d}\,\pi^{d/2}}{m\, Q} \| z^{d-1} V'(z) \|_{L^1(r_{kl}-\frac{\sqrt{d}}{m}, r_{kl}+\frac{\sqrt{d}}{m})}\,.
\end{aligned}$$

It easily follows that, for some constant $K$,

$$\frac{1}{N} \left| H_N(\sigma) - \bar{H}_M^{(0)}(\eta) \right| \le \left( \frac{4K\sqrt{d}\,\pi^{d/2}}{m} \| z^{d-1} V'(z) \|_{L^1} \right). \tag{A.X}$$

The parameter $\epsilon$ is given by,

$$\epsilon \equiv \beta \frac{4K\sqrt{d}\,\pi^{d/2}}{m} \| z^{d-1} V'(z) \|_{L^1}.$$